Magnetic Field Tomography of Hydrogen-Rich White Dwarfs

E eu vos direi: "amai para entendê-las!
Pois só quem ama pode ter ouvido
Capaz de ouvir e de entender estrelas"
— **Olavo Bilac, Via Láctea**

Author:
Adeilton Dean Marques Valois
Advisor:
Kepler de Souza Oliveira Filho
Universidade Federal do Rio Grande do Sul

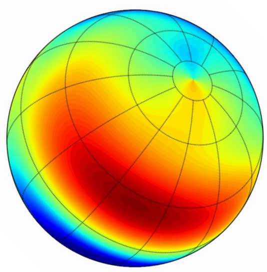

January 21st, 2018

Dedication

Quando olhamos para o céu, ao contemplar o Sol de um crepúsculo, as estrelas longínquas, as nebulosas difusas, e a Lua exuberante, nos sentimos reduzidos, inferiores. O que mais, senão o Universo, pode causar tamanho sentimento de pequenez, e insignificância? Mas o que para alguns é irrisório, para outros significa tudo, afinal importância é um conceito relativo. Para mim, as pessoas das quais falarei agora foram de suma importância para que eu chegasse até aqui hoje, e pudesse escrever estas linhas. Sem elas, eu estaria a vários kiloparsecs de ser quem sou hoje.
Ao meu orientador, Kepler, não Johannes Kepler, nem Kepler "o telescópio", mas Kepler "a pessoa", cuja fama e reconhecimento dispensam apresentações, só tenho a agradecer. Poucas pessoas que já conheci na vida esbanjam tanto conhecimento e sabedoria quanto este homem, e por isso eu o admiro profundamente. E foi com esta sabedoria que ele me orientou, e me guiou através das anãs brancas, durante meus quatro anos de faculdade. Obrigado por sempre me fazer sentir parte do grupo, por sempre nos escutar e observar com olhos atentos. Juntamente ao Kepler, agradeço aos meus amigos e amigas do grupo de anãs brancas, do Departamento de Astronomia, e do curso de física como um todo. Foram tantos os desafios que enfrentamos juntos durante quatro anos maravilhosos da minha vida, vocês me acolheram como se fizéssemos parte de uma família.
Falando em família... gostaria de deixar aqui registrada uma mensagem para pessoas muito importantes para mim. Aos meus pais, Lizy e Rubenilson, queria que soubessem que palavras tão simples em frases tão cotidianas como "bom dia, Dan" e "te amo, filhão" têm mais significado para mim do que possam imaginar, elas me mantêm firme todos os dias, sabendo que em um minúsculo pedaço do Universo sempre haverá pessoas especiais que me darão amor, carinho, e conforto. E por isso eu os agradeço, bem como ao meu tio, Laércio Golveia Demóstenes, à minha madrinha, Rosa Ribeiro Valois, carinhosamente conhecida como "dindinha", e ao meu "dindinho", João Maciel Rodrigues Jr.

Obrigado por lutarem pelos meus sonhos! Mesmo que jamais entendam o que venha a ser escrito nestas páginas, mesmo que não saibam quem é ∇, o que é um $\hbar$, ou quem foram Maxwell, Schrödinger, e Feynman, mesmo que não entendam o significado de um *bra*, de um *ket*, ou que jamais aceitem que $-\frac{\hbar^2}{2m}\boldsymbol{\nabla}^2\Psi + V(\mathbf{r},t)\Psi = i\hbar\frac{\partial\Psi}{\partial t}$, sempre foram e sempre serão vocês por trás dos meus maiores sonhos, meus sonhos mais ousados, o tempo todo. Vocês são minha fonte de inspiração, meus heróis, minha vida. Quero que saibam que eu os amo mais do que tudo no mundo.
À minha irmã... querida irmã, meus olhos ainda se enchem de lágrimas quando paro para pensar no

quanto você cresceu, e no quanto tive que sacrificar das horas que passávamos juntos, horas que nos eram tão comuns à época da infância, e que agora tornaram-se tão distantes. Infelizmente, o tempo não anda para trás (ao menos é o que dizem os físicos!), porque se o fizesse, eu daria tudo para reviver ao seu lado nossos momentos de glória. Em homenagem a esses momentos, parei para lhe dedicar estas singelas palavras. Não importa o que aconteça, você jamais deixará de ser minha irmãzinha que eu tanto amo.
À minha linda namorada, Brenda Bertotto Malabarba, obrigado por todas as horas que passamos juntos, obrigado por acreditar em mim e por me acompanhar em todas as nossas aventuras em nome da física. Você é a estrela que brilha radiante no céu dos meus dias. Eu te amo!



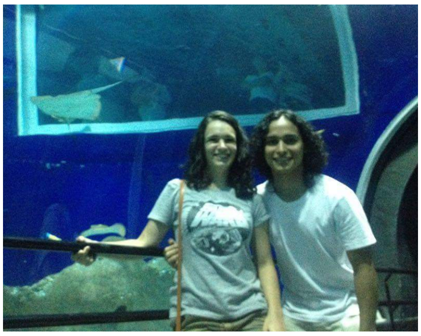

Em memória do meu avô, Laércio, que há pouco deixou para sempre esta vida, e que apesar de nunca ter acreditado num futuro entre as estrelas, não deixou de ser a pessoa que me carregou no colo, que me deu amor e conforto quando precisei, que me viu crescer, cair da bicicleta, e após ralado o joelho, levantar para me tornar quem sou hoje.

Abstract

White dwarfs are among the oldest objects in the Universe, and hold the key to understand past, present and future of nearly 95 % of all stars in the Milky Way. About 10 % of those are born surrounded by gigantic magnets with field intensities vastly ranging between low and high limits, far larger than even the fields produced in the most sofisticated devices at laboratories on Earth. Most part of the mysteries concerning these stars remain unsolved. In this work, I used a numerical fitting routing based on χ^2 minimization with pre-calculated synthetic spectra of white dwarfs with hydrogen-rich atmospheres for finding the best solutions to the geometrical configuration of their magnetic field with basically three fitted parameters: magnetic field strength (B_p), dipole off-set in the z direction ($z_{\rm off}$) and inclination of the dipole axis. This attempt was made for around 156 spectra from the data releases of the Sloan Digital Sky Survey (SDSS) with signal-to-noise ratio between $\sim$ 10-90 through a computational technique for calculating the magnetic distribution over a visible stellar hemisphere by superposing fields with a basic input geometry, represented by spherical harmonics, and with different intensities along the grided stellar surface. With the aid of a statistical hypothesis test, I analysed the solutions with distinct input geometries so first-order approximations to the magnetic topologies could be found.

Contents

Chapter 1

Introduction

"Não apenas vivemos neste universo. O universo vive dentro de nós"

— **Niel deGrasse Tyson**

For many years, magnetic fields have been considered a source of great lack in both theoretical and observational understanding in the context of stellar physics. In the frame of hydrogen-rich white dwarfs, very old stars with atmospheres dominated by hydrogen (also called DA), around 10% of their known population have been identified as encapsuling giant, strong magnets. Magnets with fields ranging between incredibly high intensity limits. From recently identified values of a few kG [Landstreet et al., 2016, Landstreet et al., 2017] up to 1000 MG [Vanlandingham et al., 2005], field belonging to the most magnetized white dwarf ever discovered. No long-lasting experiment has ever been made to study matter at so extreme conditions on Earth. However, experimentalists have invested considerable efforts in order to achieve astrophysical magnetic fields transiently in the laboratory. In 1924, Kapitza was able to reach a 10 T field (1 T corresponds to 10^4 G) lasting for 0.01 seconds [Kapitza, 1924]. During the 60's, Fowler obtained, and sustained for 2 μs, a magnetic field of 1400 T [Fowler et al., 1960]. The Large Hadron Collider, during a single proton-proton collison, can measure up to 10^{15} T, a typical field of a neutron star[1], but lasting for miserable femtoseconds (1 fs = 10^{-15} s). But it's only at stellar labs that fields of such greatness are achieved and maintained millions, billions of years across the cooling process of the dead stars called white dwarfs. One reason is that highly magnetized systems can become self-destructive as the field increases, like the implosion technique used by Mr. Fowler. You can imagine why is that so, since they start squeezing under enormous magnetic pressure (as demonstrated by Fermi and Chandrasekhar in 1953 [Chandrasekhar and Fermi, 1953]). Even stars fail to keep their spherical symmetry under the claws of strong magnetic fields [Coelho et al., 2014], for some of them look more like

[1] Actually neutron stars have even higher fields, but are so rare, faint and small that can hardly be studied in details.

oblate spheroids than like rea spheres. The magnetic tension is governed by the very simple pressure equation below:

$$P_{\text{mag}} = \frac{1}{2\mu_0} B^2 \tag{1.1}$$

Now let's see what that means. Suppose a spherical magnetized object with the size of the Earth, and a surface field of the most magnetized white dwarf known: 1000 MG. What pressure is it beneath to? Can you believe this is the pressure of $\sim 10^{10}$ Earth atmospheres? Almost an inconcievable number. And the origin of these gigantic stellar fields is still very poorly understood and remains a mystery. Many discussions concerning their unknown nature have already taken place in the literature [Tremblay et al., 2015, Valyavin et al., 2014, Gentile Fusillo et al., 2017, Wickramasinghe and Ferrario, 2005]. Such a cumbersome problem it is, that has left lots of open questions and unsolved queries, and as an attempt of studying the problems concerning stellar magnetism, I wrote these lines for my bachelor thesis.

I didn't mean to annoy you with a very long introduction, but there's really a lot that can be said about magnetic astrophysical systems, for those are the object providing the Universe with one of the richest and most exciting physical scenarios found by scientific research, and hopefully this text might be enough to convince you that. And since these stars represent a non-negligible fraction of the total white dwarf population, they deserve to be studied and well placed in the global scenario of stellar evolution. But I think I might be suspicious to say. I'm afraid to me it is inevitable to express how beautifuly these balls of flaming plasma can have so much to teach us about the very inner and the very broad branches of physics, for one can find the whole physics inside stars, from micro to macro, from the slippery neutrino emission to the highly turbulent flares, from infrared to gamma rays, from stellar winds to supernovae explosions. The big and the small, gathering within the limits of the greatest furnaces in the Universe, to build what I call the jewels that adorn the night sky.

1.1 Sloan and the several dwarfs

Sloan Digital Sky Survey[2], or SDSS, with a 2.5 m telescope at Apache Point Observatory has reached a boom in the glory of its 14$^{\text{th}}$ data release, and is the great database from where all my white dwarfs came from. It is now the biggest spectroscopic sky-covering survey of all times, and has largely improved the actual sample of stars with thousands of newly identified white dwarfs discovered every year within the different releases [Kleinman et al., 2012, Kepler et al., 2014]. Several new dwarfs have been found by our own group through visual inspection [Kepler et al., 2016b], followed by autofits with appropriate atmospheric models [Koester, 2010], covering a vast range of dominat elements, for both magnetic and non-magnetic (hereafter, normal) white dwarfs, like hydrogen (DA), helium I (DB) and helium II (DO), metals (DZ), carbon

[2] http://www.sdss.org.

(DQ), and even the so rare oxigen-dominated atmospheres (DOX) only recently glimpsed for the first time [Kepler et al., 2016a], and also the featureless spectrum white dwarfs with almost purely black-body (or planckian) continuum (DC). The magnetic extensions of these spectral types are standardly searched by looking for so-called Zeeman features (see Sec. 1.3) at the the line cores of different elements. White dwarfs are naturally blue objects because of their high effective temperatures, and because colors are affected by the presence of magnetic fields, with the blue being the most disturbed, they fall into the object search category of the SDSS, and most of their spectra were obtained with the BOSS spectrograph, disposed to massively measure galactic redshifts, with resolution in between 1560-2270 in the blue channel, and 1850-2650 in the red one, capable of taking spectra at an average range of 3600 $\AA$-10400 $\AA$. The SDSS spectra analysed here have quality limited by the signal-to-noise (S/N hereafter) interval of $\sim$ 10-90.

1.2 "D" is for Degenerate

I shall begin apologyzing myself with reference [Koester, 2015] for starting this section stealing one of its sentences that I particularly appreciate very much, which asserts that **white dwarfs are macroscopic manifestations of the Pauli exclusion principle**. I know this might sound a bit dramatic and maybe exaggerated, but believe me when I say that there's no other classification for that statement than as pure truth. White dwarfs do only exist because of the huge degeneracy pressure balancing the implacable gravitational action. With that pressure originating from all electrons' jerks in the ultra-dense and hot degenerate soap of stellar interiors, reaching temperatures from $\sim 10^6$ K to 10^9 K. And because of this atomic degeneracy, we name white dwarfs with a "D" in front of a letter that represents their spectral type, like DA for hydrogen-rich, DB for helium-rich, DZ for metal-rich, and so on. Such dense is this soap, that nearly 99% of all white dwarf mass is held by the nucleus. Yet, the photospheres enclosing these furnaces are surprisingly just as dense as the air you and me breathe while reading this line. But I haven't told you what is the photosphere. The photosphere is an outer shell of stars from which all light rays come from. As simple as that.
Because the nuclear reactions that sustains the fuel of stars in main sequence, giant, and supergiant stages have already ceased, white dwarfs are fated to cool for the rest of their lives, and the scenario in which the dynamics of white dwarfs is framed do wastes complexity, but when those stars are additionaly magnetic, this complexity is almost unbelievable, and to understand the processes by which these objects are born and evolve remains an open challenge.

1.3 “Three levels for Muster Zeeman”

Do you know the story of how Murray Gell-Mann gave the fundamental particles called quarks their name? So let me tell you in a nutshell. As a very cult physicist, he read a book by the irish dubliner writer James Joyce entitled *Finnegans Wake*, where he found a poem with a strange verse that inspired him: “Three quarks for Muster Mark”.

Obviously Pieter Zeeman didn’t read James Joyce before 1896 when he discovered the **three levels split caused by a static magnetic field in spectral lines**, but I thought it was worth it to give this section’s name. By the way, this is what Zeeman effect is all about, and **symmetry breaking** are the two simple key-words to fully understand what that boldface upside means. Although he wouldn’t have explained it using these terms, for that time there was neither quantum mechanics to support strict physical explanations, nor the electron had been discovered by J. J. Thomson.

Since Kirchhoff’s time ($\sim$1862) we know empirically how atoms behave when stimulated by external radiation sources. We would modernly say that whenever a photon of light with very specific wavelength interacts with an atom’s electron (and for the purpose of the linear Zeeman effect, a spinless electron), the former is forced to make what we call a quantum leap by absorbing this photon, creating a dark fringe pattern inside spectrographs. Each one of these dark fringes corresponds to electronic transitions with very definite energy spectrum, given by $E_n = -13.6/n^2$, where n is a number, called principal quantum number, labeling all energy levels. And as you can see, this spectrum is degenerate with respect to other quantum numbers, since only n appears. The role of magnetic field is to break this degeneracy (or break symmetry) and, in the limit of weak fields ($B \lesssim 10$ MG), it creates a three-level line profile, like the ones shown in the upper plot of Fig. 1.1, and the line components of the triplets receive names: the left one is $\sigma-$, the central (unshifted) is π and the right one is $\sigma+$. Intuitively, these three levels account

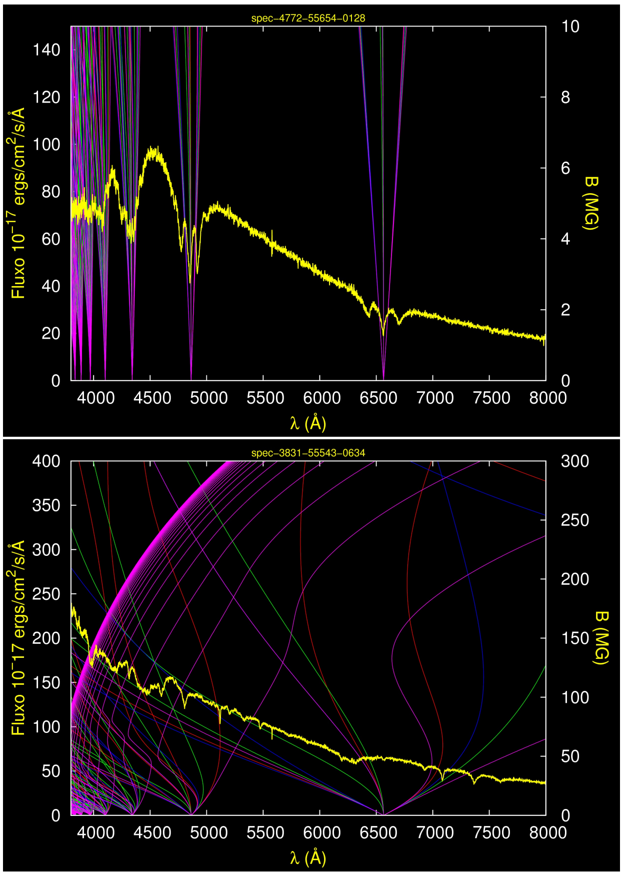

Figure 1.1: λ-B diagrams showing theoretical calculations for wavelength positions of Balmer series as a function of the magnetic field, which ranges in the linear case from 0 until 10 MG (upper plot), and until 300 MG (lower plot) in the higher order case. Observed spectra are overplotted to the curves and provide examples of weak and strong field regimes.

for the three possibilities of transition through which the electron may pass: with magnetic moment parallel, orthogonal, or anti-parallel with the field vector. The three Zeeman-splitted line components can be seen in the upper plot of Fig. 1.1 in the case of the linear regime, where perturbative theory leads to good results. In the case of the anomalous Zeeman effect (also called Paschen-Back effect), the situation becomes even more complex because the magnetic field energy is not anymore negligible in relation to the Coulomb energy, and so perturbation theory breaks downs due to the non-linear field powers on which the wavelength shift depends ($\Delta\lambda \propto B, B^2, B^3, ...$), contrasting with the 1^{st} order dependence in the normal Zeemal effect ($\Delta\lambda \propto B$). The wavelength shifts behave drastically different in the upper and lower plots of Fig. 1.1. The emergence of several other components in the non-linear case is because when magnetic fields are strong enough, one must consider the fine structure of the atom aswell, like both the spins of the electron, of the proton, and all the couplings between them, *i.e.* spin-orbit coupling, jj-coupling (for a many-electron atom), which give transitions much more freedom to happen in several different ways. For more details on the mathematical description of the linear Zeeman effect, take a look at Sec. 6.1.

Chapter 2

Numerical fits

"I sound my barbaric YAWP over the rooftops of the world"

— **Walt Whitman**

2.1 Fitting routine

The numerical task of my bachelor thesis was to do a series of automatic fits to magnetic white dwarfs' spectra in order to study their field distribution within a statistical approach (see Chap. 3). If you read the title of my work, you realized that I only deal with hydrogen-rich white dwarfs (if you didn't, go back a few pages), for these are the ones to have the biggest volume of theoretical calculations in a sense that magnetic atmosphere models can be build with good confidence, once magnetism in atomic physics has calculations available for only a few atoms (see Sec. 4.4). In order to fit my DA sample, I used the evolutionary fitting routing called YAWP [Euchner et al., 2002], which stands for *Yet Another White dwarf Program*, based on χ^2 minimization through multipolar expansions of the field topology over the visible stellar hemisphere in the basis of spherical harmonics, and on Walt Whitman's poem. By evolutionary I just mean that the code uses a fitting strategy implemented in the evoC library. The pre-calculated synthetic atmosphere models used are from D. Koester [Koester, 2010], with effective temperatures ranging from 8000 K to 40000 K[1], a limitation that brought some consequences to the fits, as shown in Fig. 2.1, and $\log g$ set as 8.0, which is the mode value for non-magnetic white dwarfs' $\log g$ distribution, corresponding to $\sim 90\%$ of the all white dwarf sample [Kepler et al., 2016b]. I know this might be a non-logical extension, since magnetic fields probably have significant effect on surface gravity calculations, but it's nowadays the best we can do. This is another consequence of our degree of ignorance concerning stellar magnetic fields' tricks, once it is not possible so far to precisely determine $\log g$ distributions in the presence of them.

[1] Actually, the original temperature interval used by the code was 6000 K - 50000 K however, to the best of my knowledge, no convergent model was obtained for fixed temperatures out of the limits in the text above.

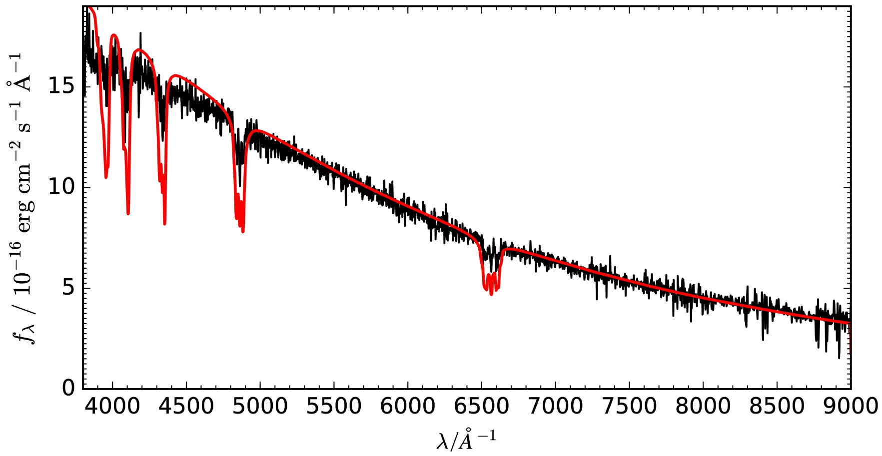

Figure 2.1: Because of temperature limitations in the models, this spectrum couldn't have its absorption lines well reproduced, eventhough the Zeeman split looks quite reasonable. The most recent temperature estimation for this spectrum has pointed to ~ 7000 K [Kleinman et al., 2013]. However, through YAWP's routine this could only be fitted with $T_{\rm eff} = 8000$ K, because even a somewhat cooler solution would not have converged. This restriction comes with the price that lines are deeper than the shallow profiles in the data.

There is not yet a well stablished study describing the systematic influence of the field in surface gravity calculations because of the highly degenerate parameter space, since a variety of other physical mechanisms are present aswell, like natural broadening, pressure broadening, Doppler broadening, etc. Moreover, the electric analogous of the Zeeman effect, called Stark effect, is dominant for fields weaker than ~ 5 MG, whose line broadening mechanism is not well understood in its full complexity for dense plasmas, and was only considered in the simple case of non-coupling between electric and magnetic fields, *i.e.* when $\mathbf{E}\cdot\mathbf{B} = 0$, at present days the only situation with which the state-of-art in atomic physics calculations provided us with theoretical data. When they couple, in the most general case of $\mathbf{E}$ and $\mathbf{B}$ enclosing an arbitrary angle, they give rise to a tough problem, where the two hamiltonian operators describing electric and magnetic field energies fail do commute. Stark broadening can be clearly stared when arising from some low-field magnetic white dwarfs since their lines become more triangular in shape, and the associated wavelength shift due to a local electric field can be estimated by the simple formula [Putney and Jordan, 1995]:

$$\Delta\lambda = 0.0192\lambda^2 n_k E \tag{2.1}$$

where n_k is an integer given by the initial and final states of the line transition, and E is the local electric field strength measured in cgs units. This electric field is responsible for the

so-called Stark broadening.
In YAWP code, absorption lines of five different principal quantum numbers can be fitted: from the Balmer α ($n = 3$) transition up until Balmer ϵ ($n = 7$). Eventhough calculations for higher n values have already been done [Schimeczek and Wunner, 2014], those were not yet implemented (λ-B diagrams of Fig. 1.1 show it for n up to 11).

2.2 The ZEBRA plot technique

ZEBRA stands for *ZEeman BRoadening Analysis*, "plot" stands for making figures. So ZEBRA plot [Donati et al., 1994] is the art of calculating the magnetic field vector within a grid subdivided into a finite number of surface elements over the visible stellar hemisphere, sketching the global structure of the magnetic field according to the local contribution of each field intensity to the final configuration, and making plots with it. In other words, basically a weighted sum of flux models in each subdivision of the stellar surface (grided into 30×60 in all my calculations) by superposing fields of different intensities. Unfortunately, there are presently no pure magnetic atmosphere models calculated by methods like in [Koester, 2010], where it solves the one-dimensional radiative transfer-equation for some photospheric layers to compute the outflow radiance, and the reason is because one cannot assume spherical symmetry, for the presence of the field turns the situation into a naturally 3-dimensional problem. There only exist 3D models via more realistic magnetohydrodynamics simulations, like the ones done by Tremblay [Tremblay et al., 2013] with his non-adiabatic program called CO5BOLD. However, these numerical simulations (for only a few kilometers of a plane-parallel atmosphere) are extremely costful, and demand a lot from supercomputers' hard work, therefore too expensive to be used for building an extensive model grid. The 3D version of the radiative transfer-equation without an external field is shown below:

$$\frac{1}{c}\frac{\partial I_\nu}{\partial t} + \hat{\Omega} \cdot \boldsymbol{\nabla} I_\nu + (\kappa_\nu^s + \kappa_\nu^a) I_\nu = j_\nu + \frac{1}{4\pi}\kappa_\nu^s \int_\Omega I_\nu d\Omega \tag{2.2}$$

where I_ν is the radiation intensity for a frequency ν, j_ν is the emission coefficient, while κ_ν^s and κ_ν^a are respectively the scattering and absorption opacities. They measure the power of a certain layer to block radiation with frequency ν by either scattering or absorbing it. So what YAWP does is to use this ZEBRA strategy to disturb D. Koester's models as if they were magnetic. The contribution of each field to the surface elements is computed and stored as measurements called filling factors, and shown in a plot of the magnetic field intensity (B) against the cosine of an angle ψ ($\cos\psi$), which is the angle between the local magnetic field vector and the line of sight. Fig. 2.2 below shows both the atmospheric model, as red line, and the field's distribution, as grey scale:

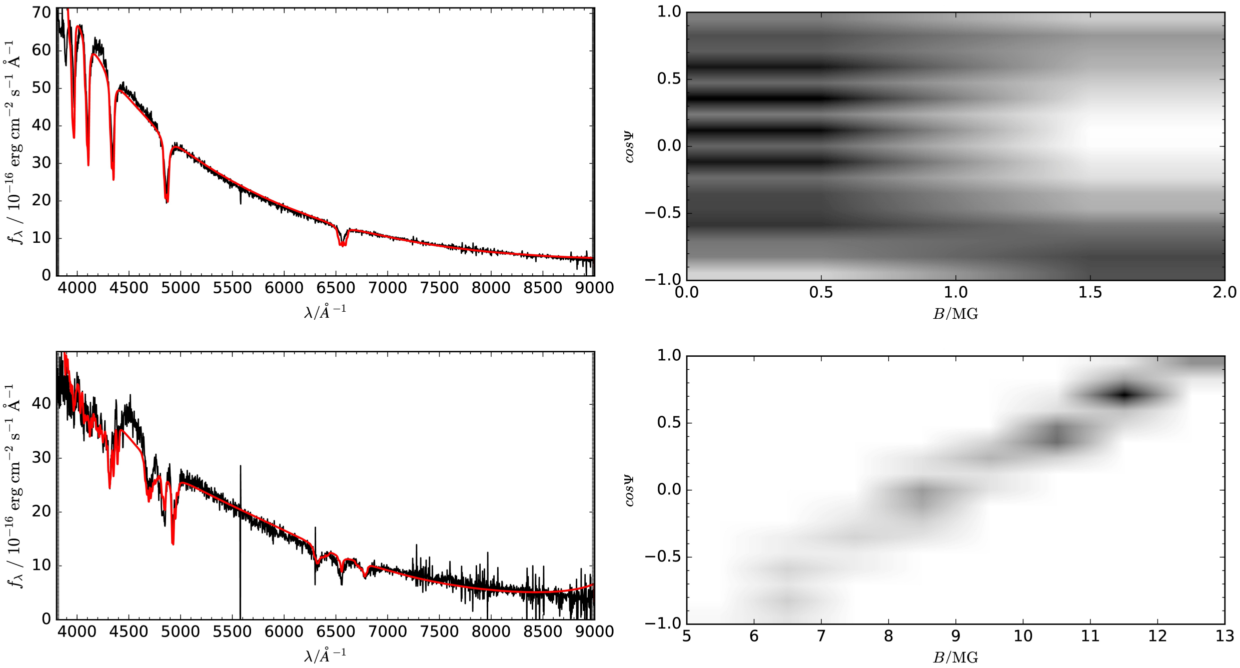

Figure 2.2: Synthetic atmosphere models and ZEBRA plots for two SDSS spectra: 4901-55711-0358 (upper plots) and 0733-52207-0522 (lower plots). The top right plot can be interpreted as a quite uniform field distribution, eventhough field strengths up to 2 MG have been used to buid its magnetic profile. The bottom right plot shows a more concentrated field, where the average is found nearly 11.5 MG.

2.3 Spherical harmonics

If you let me, I'd like to start this discussion with a very powerful statement: **spherical harmonics form a complete set!** This simple assertment holds the foundations of the method used in this work, and it means that, having a sufficient (maybe infinite) number of these spherical harmonics, every function of angular coordinates, say $f(\theta, \phi)$, carries a unique expansion within their basis set, following the general expression:

$$\boxed{f(\theta, \phi) = \sum_{l=0}^{\infty} \sum_{m=0}^{l} (a_{lm} \cos m\phi + b_{lm} \sin m\phi) P_l^m(\cos\theta)} \tag{2.3}$$

where θ, the polar angle, is enclosed by the position vector and the z-axis, and runs from 0 to π, while ϕ, the azimuthal angle, is enclosed by the projection of the position vector in the xy plane and the x-axis, running from 0 to 2π. Of course this is just a natural three dimensional generalization of the Fourier series expansion, which holds in two dimensions. However, this is not yet written in terms of spherical harmonics, there are only separated sines, cosines, and associated Legendre polynomials. But the reader may deduce that Eq.(2.3) is equivalent to an equation directly expressed in terms of spherical harmonics themselves:

$$\boxed{f(\theta,\phi) = \sum_{l=0}^{\infty}\sum_{m=-l}^{l} c_{lm} Y_l^m(\theta,\phi)} \tag{2.4}$$

Please, notice the subtle difference that in Eq.(2.4) m runs from $-l$ to l, while in Eq.(2.3) it starts at zero. Both formulae cover all zonal ($m = 0$) and tesseral ($m \neq 0$) components. And Eq.(2.3) is a lawful expansion of f in terms of spherical harmonics. But I still haven't told you how these functions look like. Actually both $Y_l^m(\theta,\phi)$ and $P_l^m(\cos\theta)$ are mathematicaly very similar, they are connected by a phase shift and a normalization factor[2].

$$Y_l^m(\theta,\phi) = (-1)^m \sqrt{\frac{(2l+1)(l-m)!}{4\pi(l+m)!}} P_l^m(\cos\theta) e^{im\phi} \tag{2.5}$$

When evaluated in the surface of a sphere, the magnetic field becomes a vector function of the angular coordinates only, which makes it perfect for being represented by spherical harmonics. To expand magnetic fields in this basis means to find the most representative components that can possibly describe their global structure. However, to stay with all expansion terms is useless, for there would be no advantages since we pay a costly price in CPU time, that's why we generally truncate it by only keeping terms of centered dipole ($l = 1$, $m = 0$), quadrupole ($l = 2$, $m = 0$), and octupole ($l = 3$, $m = 0$) fields. Furthermore, we are often interested in the overall appearence of the field, not in the fine details. From classical electrodynamics, one can easily demonstrate that the cartesian components of dipole, and quadrupole terms are given by (as modified from [Putney and Jordan, 1995]):

dipole with off-sets

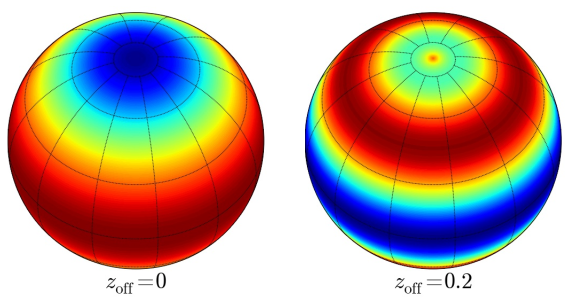

$$B_x^d = \frac{3}{2} B_p (x - x_{\text{off}})(z - z_{\text{off}}) \tag{2.6}$$

$$B_y^d = \frac{3}{2} B_p (y - y_{\text{off}})(z - z_{\text{off}}) \tag{2.7}$$

$$B_z^d = \frac{1}{2} B_p [3(z - z_{\text{off}})^2 - 1] \tag{2.8}$$

[2] This normalization factor may be defined in different ways depending on the area of application. So don't worry if you find another factor elsewhere. The way I defined above is often used in quantum mechanics.

quadrupole with off-sets

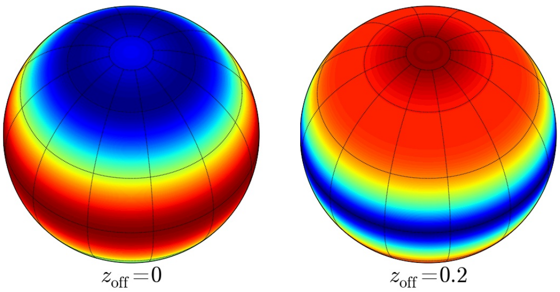

$$B_x^q = \frac{1}{2} B_p [5(z - z_{\rm off})^2 - 1](x - x_{\rm off}) \quad (2.9)$$

$$B_y^q = \frac{1}{2} B_p [5(z - z_{\rm off})^2 - 1](y - y_{\rm off}) \quad (2.10)$$

$$B_z^q = \frac{1}{2} B_p [5(z - z_{\rm off})^2 - 3](z - z_{\rm off}) \quad (2.11)$$

where B_p is the polar field strength, and the stellar radius is taken as unitary ($r \equiv 1$). The vector $(x_{\rm off}, y_{\rm off}, z_{\rm off})$ points out the position of the dipole center. In the equations above, x, y, and z are dimensionless variables measured in fractions of the stellar radius. These coordinates are called off-sets. If you've checked the previous reference by A. Putney and S. Jordan, you noticed that the authors present Eqs.(2.9), (2.10), and (2.11) without the off-sets. However, we can naturally introduce them by simply applying a coordinates transformation of the type: $x \to x - x_{\rm off}$, $y \to y - y_{\rm off}$, and $z \to z - z_{\rm off}$. And it is quite easy to imagine what do these off-set do to the field. They simply displace the magnetic axis by some constant amount along its correspondent coordinate, causing an intensity difference between north and south poles.

2.4 (Beyond) simple dipoles

There are two reasons I would evoke to argue that dipole components may be present when describing the field geometry of a magnetized spherically symmetric object, one is mathematical and the other is physical.

Since simple centered dipoles represent linearity in spherical harmonics expansion, they shall be a good approximation to the field geometry just like linearized forms of Taylor series are fine low order representations of some complex functions in ordinary calculus. We might then be allowed to replace some puzzling field topologies by their truncated harmonic expansion. But one can always ask why would we expect stars to have this first term. And that's when comes the next (physical) explanation. As stars rotate around their axis, the spherical symmetry to which its structure is restricted naturally induces the emergence of a dipole field component, since dipoles are also spherically symmetric and therefore invariant under azimuthal transformations. To sound this a bit less technical: if you see a dipole field, like in a magnet, and spin it around its axis, it will look exactly the same before and after the rotation. Although quadrupoles and octupoles with $m = 0$ are also spherically symmetric, they are higher order components and thus more difficult to be found alone in stellar fields. Moreover, there's another characteristic with which dipoles are privileged. We expect to notice more frequent incidences of dipole components because stellar dipoles decay within $\sim$ 0.01-0.1 trillion years, while quadrupoles do it ten times faster than dipoles, and octupoles ten times faster than quadrupoles [Mestel, 1965, Chanmugam and Gabriel, 1972]. So the last two components had more time to fade away than the dipole one.

Sometimes it turns out that these simple dipoles may not be the most appropiated geometries for modeling some complications that may arise in certain white dwarf's fields. And it has been a very popular practice to include the so-called off-sets in the mathematical description of stellar fields. The advantage of introducing off-sets for modeling is as follows: given the completeness of the spherical harmonics' basis, it can be used to expand whatever functions in the θ-ϕ space. In particular, it is possible to describe an off-centered dipole (say in the z-axis), just by summing up a few centered dipole and quadrupole terms. In other words, an off-set summarizes information from all these terms within one single parameter (z_{off}). So smart you are then to prefer fitting z_{off} instead of those few dipoles and quadrupoles. Besides, you probably noticed from the plots above that off-centered dipoles and centered quadrupoles are overall very similar. But whether a mathematical model makes the minimum sense in a physical context is another issue that deserves attention. Off-sets are not merely mathematical tricks to make things work, they are actually found in Nature among great astrophysical magnets, and the good thing is that we don't need to go farther than roughly 19 AU from the Sun towards the outskirts of the Solar System, to find an interesting example of how these off-sets manifest themselves. Take, for instance, the case of Uranus, a faint blue-colored planet (a pale blue dot, Carl Sagan would have called) from the famous group of the so-called ice giants, holding the fourth-largest mass, the third-largest radius, but surely the most intriguing peculiar magnetic field of all, for Uranus was gifted with 59$^{\text{o}}$ of inclination between the magnetic and the rotation axes, and 1/3 of stellar radius in off-set. A lot can be questioned concerning both these numbers (questions that will soon motivate us for discussing the context of white dwarfs), because neither the rotation axis, nor the magnetic one present any alignment with their fellow planets in the Solar System. The Sun and the Earth have both magnetic fields, probably off-centered magnetic fields, although not so "off" as in Uranus case.

Besides Uranus, there are two kinds of magnetic main sequence stars called Ap and Bp (the "p" means that their a magnetic field was identified through polarimetry techniques) that are also very well adjusted with the inclusion of these off-sets, and because of their brightness, even higher order poloidal field components, *i.e.* spherical harmonics with higher l and m values, can be identified through tomography methods, and so the field distribution can be extensively mapped, as done in very recent works [Rusomarov et al., 2017]. Also, because of their off-set intrinsic characteristic, there is a wide discussion of whether these... No! Not the time for it, better leaving it to Sec. 4.3.

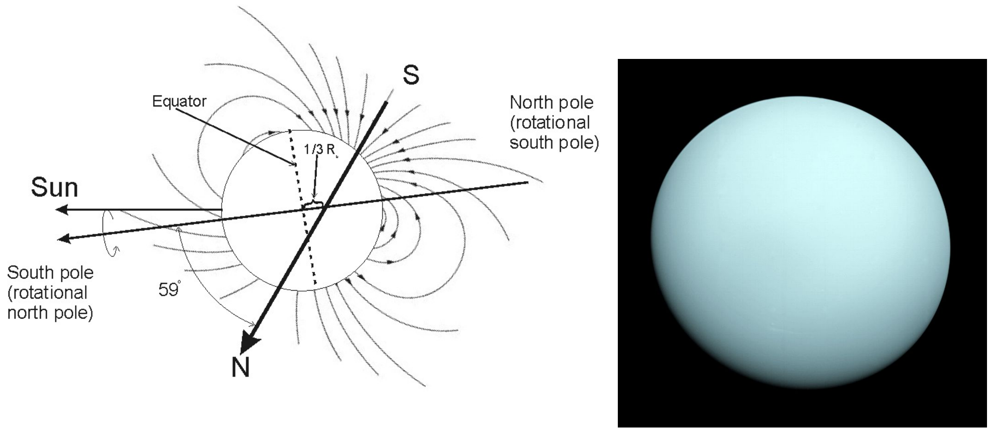

Figure 2.3: Schematical plot of the so peculiar magnetic field of Uranus (right plot), with 59º of inclination with respect to the rotation axis and an off-set measuring 1/3 of its radius.

2.5 Quadrupolar field

Although most of the fits done here had dipole fields as input, YAWP allows the user to combine a vast number of different geometries (nearly 15) to model the spectra. And sometimes it happens that dipoles are not enough to fully explain the observed spectrum. If this turns out to be the case, fine! Then we appeal to the next spherical harmonics component, truncating the expansion in the quadrupole term. Some authors have already reported the discovery of white dwarfs' fields not only inheritors of a quadrupole component, but also dominated by it [Euchner et al., 2005]. And as an example of a dipole+quadrupole fit, I present in the next figure the interesting case study of the star PG 1015+014, whose highly resolved spectrum has the PMF code[3] 3831-55543-0634, and S/N equal to 82 in the Sloan g-band, one of the bests I have. This spectrum showed visually a very good quadrupole fit with dominant quadrupole strength (B_q) over the dipole one (B_d), in three different situations for the polar angle between the quadrupole and the dipole (θ_q). The three cases shown in Fig. 2.4 are, from left to right: $\theta_q = 0^o$, $\theta_q = 45^o$, and $\theta_q = 90^o$. The ZEBRA plot pattern presented by these fits seem to strongly deviate from simple dipole profiles.

2.6 Higher order multipole terms

For even more complex field topologies, higher order poles of spherical harmonics, other than dipoles and quadrupoles, may be present. However, one should be very careful when searching for these terms because they may not represent correctly the physical reality of the

[3]PMF is the Sloan way of identifying spectra in their catalogue. "P" stands for Plate, "M" stands for Modified Julian Day (MJD), and "F" stands for Fiber.

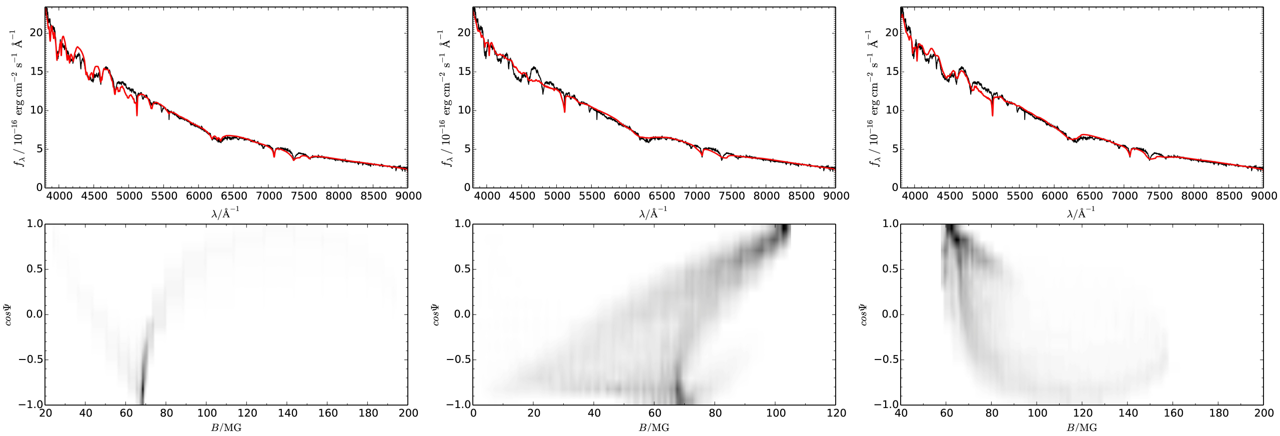

Figure 2.4: From left to right, the χ^2 values for these fits are: 0.711 (left), 0.748 (middle), and 0.773 (right). The strength of its quadrupole field, in the best fit run, was approximately 110.9 MG, while the dipole one 83.5 MG.

star's magnetic field, since you may be overfitting the data (see Chap. 3). Imagine, for instance, that a certain ideal star can have its field configuration divided into two branches, *i.e.* a spot covering half of its surface. This is basically a centered dipole where a side of the spot is the north pole while the opposite one is the south pole. This hypothetic field geometry needs nothing more than one spherical harmonics component to be fully represented, from Sec. 2.3 this is: $Y_1^0(\theta, \phi)$. Now, suppose that this spot contracts and does not occupy half anymore but, say, 1/10 of the visible hemisphere. This time, this little spot needs nothing less than an infinite number of spherical harmonics components to be fully represented! But does this mean that the little 1/10 in size spot is a more complicated field structure than the half-sized spot is? Of course not! When I realized that, many things started to make sense for me. It's important to have in mind that having more spherical harmonics terms doesn't necessarily mean to be more complex, for that is just a consequence of the spherical basis we are using.

Now I would be happy to discuss with you some of the problems arising from the numerical fits I have done. Those are unavoidable problems that would come from any standard fitting routine all the same. In order to understand what are they all about, it is substantial to first revise some fundamental concepts of least-squares fitting[4]:

2.7 χ^2 minimization

The very goal of a least-squares fitting routine is to find a good solution for a certain set of data within an iterative process, and in the context here, "good" means with minimum

[4] Although the method presented in Sec. 2.7 is not the one implemented in YAWP code, I find it useful for the sake of catching up with the basics.

errors, using the least number of parameters. Given a set of (N) measurements $\{y_1, y_2, ..., y_N\}$, and a function of, say, n parameters $f = f(x; \mathbf{p})$, where $\mathbf{p} \equiv (p_1, p_2, ..., p_n)$ is the vector with components given by the parameters of our model f, we can define a residual as $r_j \equiv y_j - f(x_j; \mathbf{p})$, and then sum over all measurements taking the square of each residual: $\sigma \equiv \sum_j r_j^2$. For the code used here is based on minimizing residuals, we need to set derivatives of σ with respect to all parameters as zero. First, we take the derivative of σ with respect to the k-th parameter as zero:

$$\frac{\partial \sigma}{\partial p_k} = \frac{\partial}{\partial p_k}\left(\sum_j r_j^2\right) = \sum_j 2 r_j \frac{\partial r_j}{\partial p_k} = 0 \tag{2.12}$$

as there are n free parameters in the model f, Eq.(2.12), iterated over all k, is equivalent to a set of n conditions of minimization, *i.e.* n gradient equations, which can be summarized in compact notation, if we use the previous definition of parameters vector, as:

$$\frac{\partial \sigma}{\partial \mathbf{p}} = \mathbf{0} \tag{2.13}$$

Once σ depends upon all components of $\mathbf{p}$, in parameters space it defines a n-dimensional surface: $\sigma = \sigma(p_1, p_2, ..., p_n)$. Usually many-dimensional mainfolds have lots of local minima, but hopefully one global minimum. As an intrinsic characteristic of multidimensional fits, there's no way to get rid of all local minima and correctly guess what is the true global minimum. However, there's a tricky way of smoothing this problem: do the minimization proceedure many times, with different sets of start-up parameters! This is a golden rule for multidimensional fits. Nevertheless, be aware that it won't give you confidence that you in any time really achieved the global solution, but will probably help you to discard local minimum solutions. To make you understand it better, I have though of a simple experiment: suppose you are invited to play a game in a dark room filled with buckets. There are dozens of blue-colored buckets, but, let's assume, a unique red one. Your goal is to kick the red bucket, but whenever you kick a blue bucket, the game starts all over again. What should you do to maximize your chances of winning the game? Try playing it many times, starting each time in a different place at the room. This would crucially increase your probability of having stumbled in a red bucket during one of the shots. Just below, in Fig. 2.5, there are three distinct runs for the one spectrum with PMF code 0437-51869-0369, and with the same set of parameters, now turning to the real problem, that show of why this game shall be played.

This star has been a case of investigation, since there's no consensus among authors about the spectral type of this object. It could be either a magnetic star with such high field that almost all absorption lines were spread out along the continuum level, or a DC star (see Sec. 1.1). But the thing is that we have no solid evidences to prefere one rather than the other, and that's the reason why I have done several fits for it. The local minima problem arrived when I tried models with fields between 100 and 500 MG, as a hunch for the interval of its field intensity due to the very shallow lines in the spectrum, although the runs showed that the best

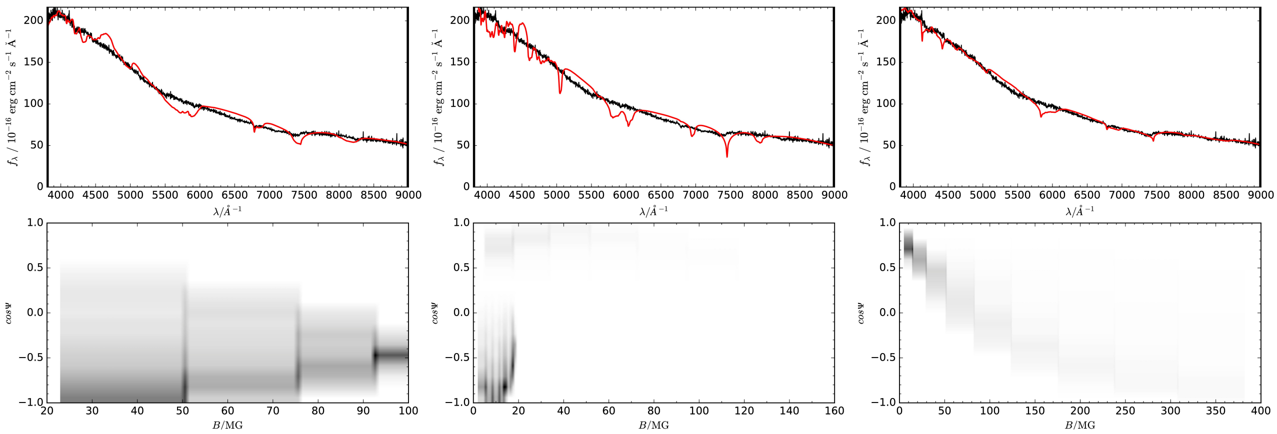

Figure 2.5: Three completely different solutions for this star with exactly the same free parameters within three runs. Top plots show the calculated synthetic spectra, while bottom plots show ZEBRA features of each magnetic field configuration. A good illustration of the local minima problem. For this reason the code was ran many times so it doesn't get stuck in local minima.

solution to this spectrum was not within these field limits. Instead, the best solution was found between 50 and 100 MG, where no local minimum was found. More precisely an off-centered dipole with field of ~ 65 MG, an off-set of $z_{\rm off} \approx -0.3$, and inclined by $i \approx 1.4^{\rm o}$ showed to be the best global solution, as shown in the figure below:

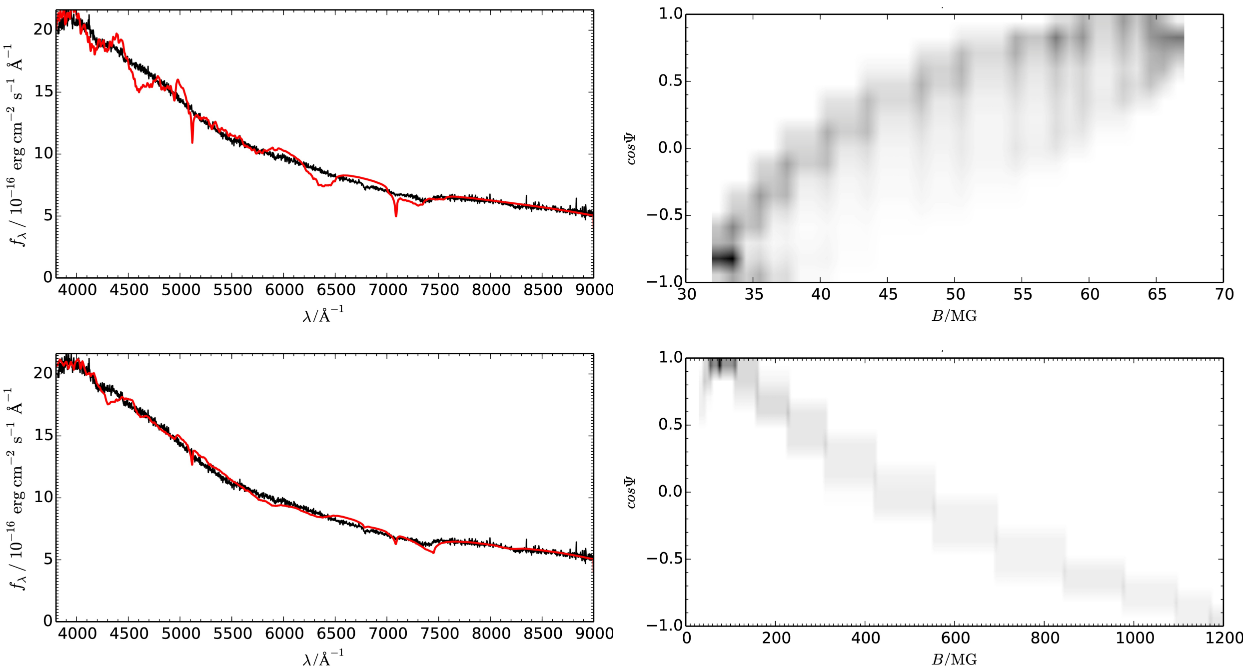

Figure 2.6: Both centered (upper plot) and off-centered (lower plot) dipole solutions for the spectrum 0437-51869-0369. In the first case, the best-fit parameters were: $B_p \approx 67.0$ MG, $i \approx 34.9^{\rm o}$, and in the second: $B_p \approx 65.0$ MG, $z_{\rm off} \approx -0.31$, $i \approx 1.4^{\rm o}$. Notice that the centered dipole does not reproduce the spectrum at all.

Chapter 3

Statistics and data analysis

"There are lies, there are damn lies, and then there are statistics"
— **Mark Twain, Chapters from My Autobiography, 1906**

It might have seem at first a little bit contradicting to write a chapter about statistical analysis after reading Mark Twain's quote above. But don't be so bothered by that. Throughout the next pages I'm going to show how this important technique helped me (and hopefully will help you) to understand what all those numerical fits in Chap. 2 want to say about magnetic white dwarfs sample and their field structure. Although very powerful, some care is needed when dealing with statistics. First of all, the reader must be aware that the motivation for using it as an analysis tool is that in this work there were different kinds of models which should be compared in order to decide which one is the most profitable. And so I needed some formal way of saying "this model produces significant quality improvement because of this, and that". That formal way is presented in the next section. However, by no means this method provides us with absolute answers. Thinking about the famous, and hard-spelling, *gedankenexperiment* of a non-skewed coin: even if you through it one billion times you could never guess what will be the next result at all[1], for statistics is not absolute. Science is not absolute.

3.1 The statistical F-test

Within the classical theory of probability, the so-called F-test can have different formulations. But in all cases, the test consists of comparing the variances of two models fitted over a sample data in order to check whether one's variance change is statistically significant when compared

[1]In principle you could, if you were able to know all significant forces acting on the coin at the moment you threw it, but let's assume this is a perfectly random process.

to the other. And I have just said the key-word for the correct use of statistics: **significant**. Inside statistical formalism, there's no better or worse model, for one could find a "perfectly" fitting model, with arbitrarily low χ^2, but terribly any prediction power, just by inserting a sufficient number of free parameters. A phenomenon called **overfitting**. Do never overfit something if you are up to an important work, like a paper, or a bachalor thesis. Usually those models have different number of parameters, say p_1 and p_2, with $p_2 > p_1$. The comparison is made through the so-called **F-statistic**, defined by the following equation:

$$\boxed{F \equiv \left[\left(\frac{v_1}{v_2}\right)\left(\frac{N_{\text{eff}} - p_1}{N_{\text{eff}} - p_2}\right) - 1\right](N_{\text{eff}} - p_2)} \tag{3.1}$$

where v_1 and v_2 are the variances of models 1 and 2 respectively, and N_{eff} is the total effective number of independent data points in the sample. And for reasons explained later, N_{eff} is usually smaller than the total number of available data points. The way we calculate variances follows the standard formula below:

$$v = \frac{1}{N-1}\sum_{j=1}^{N}[f(x_j) - y_j]^2 \tag{3.2}$$

The F-test is achieved when we compare this calculated value for the F-statistic with the F cumulative distribution, whose mathematical formula is given by the integral over the random variable x from 0 to F, given by Eq.(3.1), of the F-distribution. Thus we write:

$$\boxed{P(F; d_1, d_2) = \frac{1}{\beta(\frac{d_1}{2}, \frac{d_2}{2})}\left(\frac{d_1}{d_2}\right)^{\frac{d_1}{2}} \int_0^F dx \left(1 + \frac{d_1}{d_2}x\right)^{-\frac{d_1+d_2}{2}} x^{\frac{d_1}{2}-1}} \tag{3.3}$$

where β is the Euler's beta function, d_1 and d_2 are the degrees of freedom of both models, calculated through: $d_i = N_{\text{eff}} - p_i$. Here p_i is the number of free parameters of the i-th model. And to Eq.(3.3) we can afford a very simple interpretation:

the cumulative distribution gives the measurement concerning a theoretical probability of the variance change not be due to randomness.

Now it's worth it to highlight that I didn't use N_{eff} as the total number of data points (N) available in a typical Sloan spectrum, which is $\sim$ 3000-5000, due to the fact that one single fiber at Sloan's telescope generates on average three flux measurements, an effect called **astronomical seeing**, and it causes a twinkling in the image of astronomical objects because of turbulent mixing on Earth's atmospheric fluid. So not all points in the data are totally uncorrelated. On average, like I said! Meaning that this number might be different for each individual object caught by the spectrograph, depending on the available resolution. That's why I adopted a correction factor of 1/3 for calculating N_{eff}, performing the F-test, and thus

making my conclusions, reducing to $\sim$ 1000-2500 the effective number of independent data to be used as input in Eq.(3.1). This relates N_{eff} and N by: $N_{\text{eff}} = N/3$. If the number 1/3 isn't friendly to you, feel free to choose any other correction factor that satisfy yourself, as long as you have a good reason to explain the origin of your factor.
By applying this method to the white dwarf sample used in this work, we discover that, for the sake of describing their field structures, off-sets proved to be essential in most cases (read it in more details in Chap. 5). The plots in Fig. 3.1 show examples of runs for different spectra of both centered and off-centered dipole models:

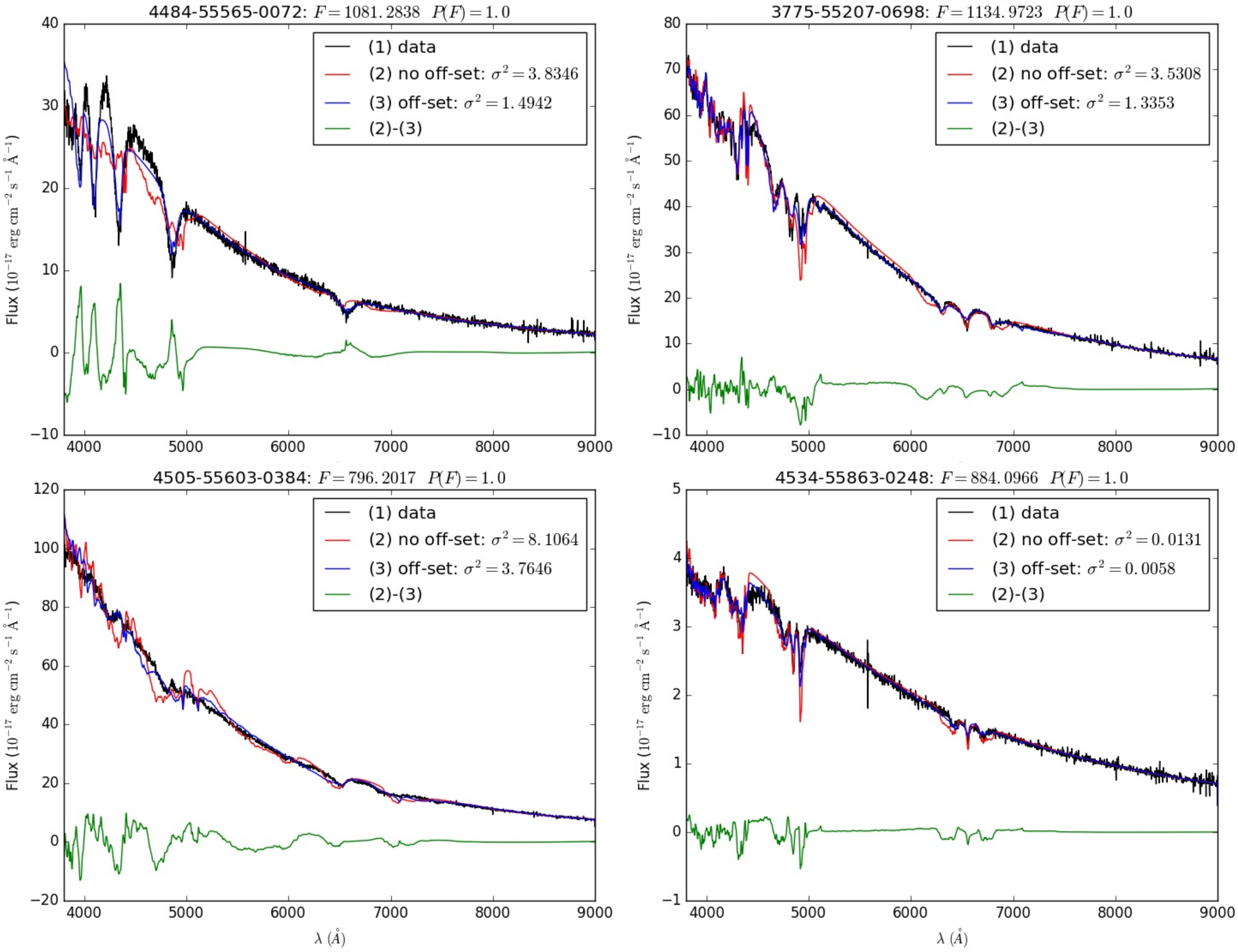

Curiously, the subtraction between the centered and the off-centered dipole solutions gives rise to patterns of downward bumps below the zero-flux line (as shown by the green solid lines), which means that an off-set commonly plays the role of decreasing line depths in the models, that are often overestimated by centered dipoles, an outcome that mimics the role of scaling the effective temperature. Because temperature generally controls the depth of absorption lines.

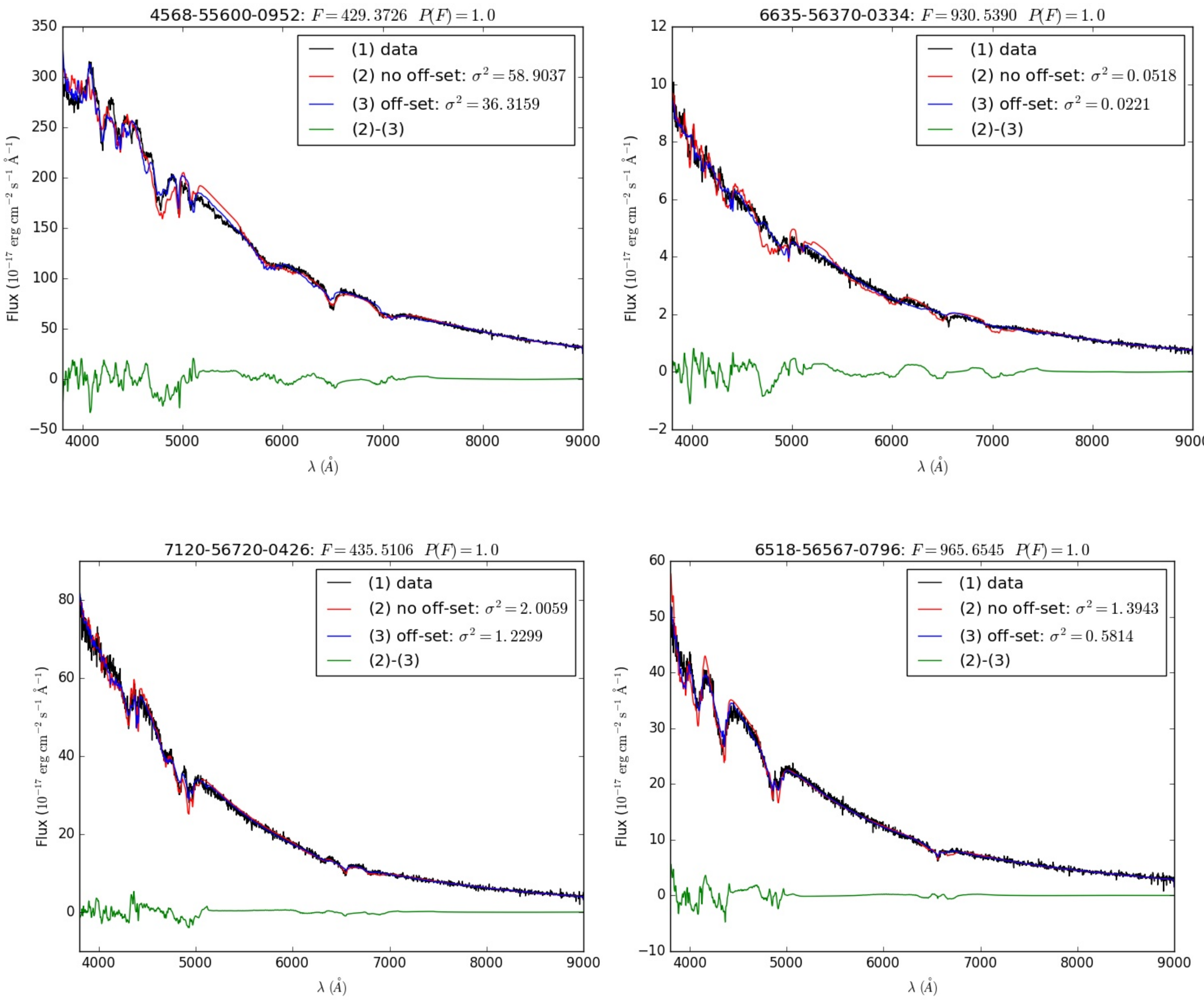

Figure 3.1: The plots of two distinct geometry models for 8 different spectra. Red lines show centered dipole best fits, while blue lines show off-centered dipole best fits. Green lines were obtained by subtracting the blue from the red.

This characteristic makes the off-sets quite malleable for adjusting models to the data. Notice also that some spectra couldn't even be confidently reproduced by centered dipoles as input geometries, the case of 4484-55565-0072 (top left-hand corner) is the most dramatic one. For those cases, I had calculated high values for the F-statistic, leading to $P(F)$ very close to unit, as presented in the titles of the plots. Which means that the theoretical probability of the fit improvement be significant is almost 100%. The output parameters for all spectra fitted in this work may be found in Sec. 6.2.

Chapter 4

Unsolved problems

> "Somewhere, something incredible is waiting to be known"
>
> — **Carl Sagan**

If I would dispose myself to write about the whole sample of problems concerning stellar magnetism, as large as it is, this would be one of those several-page chapters that nobody (except me) would have pacience to read. Don't worry, for this is not the case! However, if you do find yourself interested by this subject, you are refered to a very good and broad review about magnetic white dwarfs: [Ferrario et al., 2015]. Moreover, I consider of astronomical importance (and of crushing interest aswell) to present here some of the "pain in the neck"'s that were faced during my period of work with this issue.

Talking about period, I have just remembered something that deserves to be remarked. Magnetic fields have some kind of power to broad, increase, or enlarge the values of measured quantities in relation to normal white dwarfs. What I'm saying is that when we compare parameter determinations between non-magnetic and magnetic white dwarfs there is a subtle difference which bias for increasing in the former case. Take, for instance, the rotational period range at which magnetic white dwarfs are found. White dwarfs with magnetized atmospheres may be noticed to belong to a much broader interval, for they can have rotating times of a few seconds to hundreds of years [Koester et al., 1998]. This is one of those things in our big list of what is not very clear yet, but If I had to give it a shot, I would guess that this might be related with the fact that magnetic field lines may grab tightly the expelled material from the star when (or if) it passes through a planetary nebula formation process[1]. Not only periods are victims of magnetic fields' endless tricks, for masses do also seem to be affected, and a

[1] I personaly prefer the "when" rather than the "if" because it sounds more elegant to say: "one day all white dwarfs will shine as bright as the so beautiful planetary nebulae" right after sweeping the outer shells, but the sad truth is that we are not sure about the total fraction of them that really undergoes a planetary nebula stage.

very rigorously-followed law that restricts them, violated! The average mass of normal white dwarfs is calculated as being $\sim 0.6\ M_\odot$ [Kepler et al., 2016b], while for the magnetic case it is slightly higher: $\sim 0.8\ M_\odot$. And besides these two, the cooling times for magnetic stars are also supposed to be longer because of the very likely suppression of convective processes in even moderate field intensities [Gentile Fusillo et al., 2017].

One intriguing problem that haunted me during the happy hours I spent with magnetic white dwarfs was a sort of behaviour found in some spectra that we initially though to be a somewhat rare phenomenon. Or at least I did. However, time has shown us dozens of spectra with this peculiarity, promoting it to a more incident occurence, other than a rare one. This problem incited me to start a project and ask for telescope time at LNA (*Laboratório Nacional de Astrofísica*) in order to study it with additional photometric data. Unfortunately the observations from that project, although successfuly approved by the LNA committee, won't come in time to be carved through this lines. OK! I know you might be curious to discover what is this problem all about, but before exposing it here, let me first review typical hydrogen line profiles in a magnetic white dwarf:

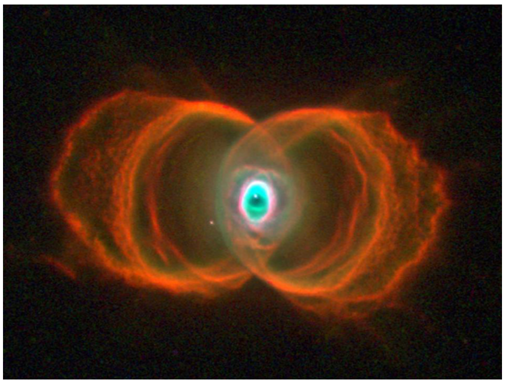

Figure 4.1: I don't want to make your mind or be biased for you to believe in the theory that says magnetic fields are behing the exuberant shapes of planetary nebulae, but I do clearly see here something that resembles a dipole. Don't you?

4.1 No ordinary stars

The spectra of Fig. 4.2 below show ordinary Zeeman spliting within approximately linear regime of fields. Notice that from Hα to Hγ the line profile continuously change its shape, passing from the classical well defined Zeeman triplet refered in Sec. 1.3 to a more complicated pattern of irregular components. This because the split of line components depends on the number of possible channels by which the electron can go from one level to another within a transition process.

The Balmer α transition occurs when an electron travels from $n = 2$ to $n = 3$ quantum states. Remembering quantization rules, it turns that l, the orbital quantum number is such that $l < n$, and the azimuthal quantum number is restricted by $-l \leq m \leq l$, which gives $2l + 1$ possibilities for m. However, at first order approximation, only transitions respecting some specific selection rules are allowed. For 1$^{\text{st}}$ order transitions, those are: $\Delta l = \pm 1$ and $\Delta m = 0, \pm 1$.

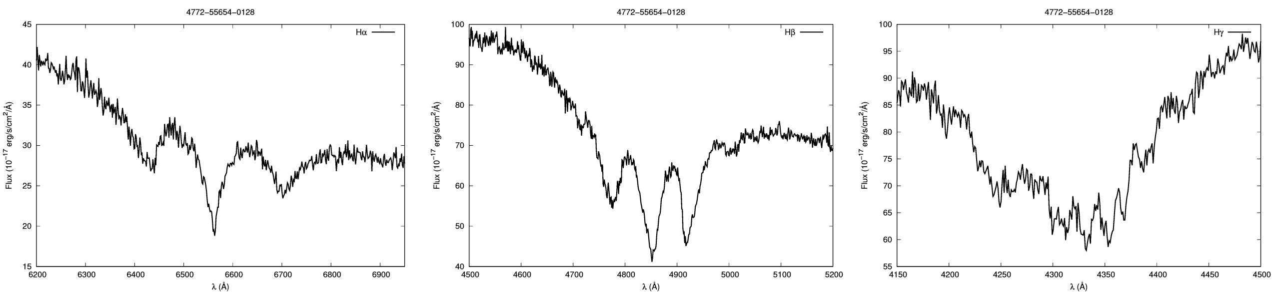

Figure 4.2: Plots of Hα, β, and γ of the same spectrum 4772-55654-0128 showing clear Zeeman splits due to a $\sim$ 11.6 MG field.

This is theory, in practice complications and exceptions may arise, as it is the case of an interesting star SDSS J030407.40-002541.74, a big name that, for simplicity, we may abreviate for J030407 hereafter. This star showed an intriguing uncommon behaviour in the $\sigma-$ component of the Hβ line. The series of spectra below illustrate how this component changes with time as the star rotates, becoming more pronounced and then completely vanishes, while the other components seem unvariable. The first question to be made was naturally concerning the timescale of these changes, how fast does this star have its $\sigma-$ component disappeared, for it may contain information about the variation of the local magnetic field configuration in the visible side of the star. Magnetic white dwarfs are known for being objects with intrinsic variability [Brinkworth et al., 2013, Valeev et al., 2017] as a result of the interaction between the outcoming light and the field.

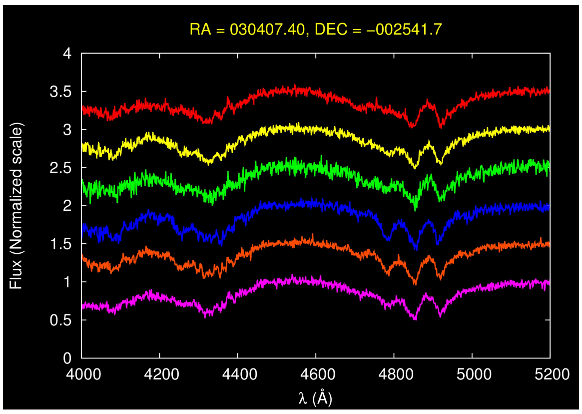

PMF	Date of observation
0411-51873-0172	Sun 02/03/2008 21:38:53
0411-51817-0172	Sun 02/03/2008 17:31:46
0411-51914-0169	Wed 27/02/2008 21:06:26
0710-52203-0311	Mon 25/02/2008 18:46:29
0709-52205-0120	Mon 25/02/2008 18:36:05
2048-53378-0280	Sat 09/02/2008 23:11:07

Table 4.1: Observation dates for J030407 with its 6 SDSS spectra.

Figure 4.3: The six SDSS spectra for J030407 showing clear time variations in the Hβ's $\sigma-$ component. This phenomenon is yet not explained by any particular field configuration of our models. From top (red spectrum) to bottom (pink spectrum), the spectra's PMFs are listed in Tab.4.1

For very obvious reasons, I like to call this problem a "Hβ defficiency". However, J030407 isn't the only one to present intriguing behaviours, but she was the first star to be found with

Hβ-defficiency. There are some other spectra that clearly present the same characteristics. And a even more dramatic case happens with the spectra of J163036, for which magnetic variability is so pronounced that the whole Balmer series changes from one spectrum to the other, as shown in Fig. 4.4.

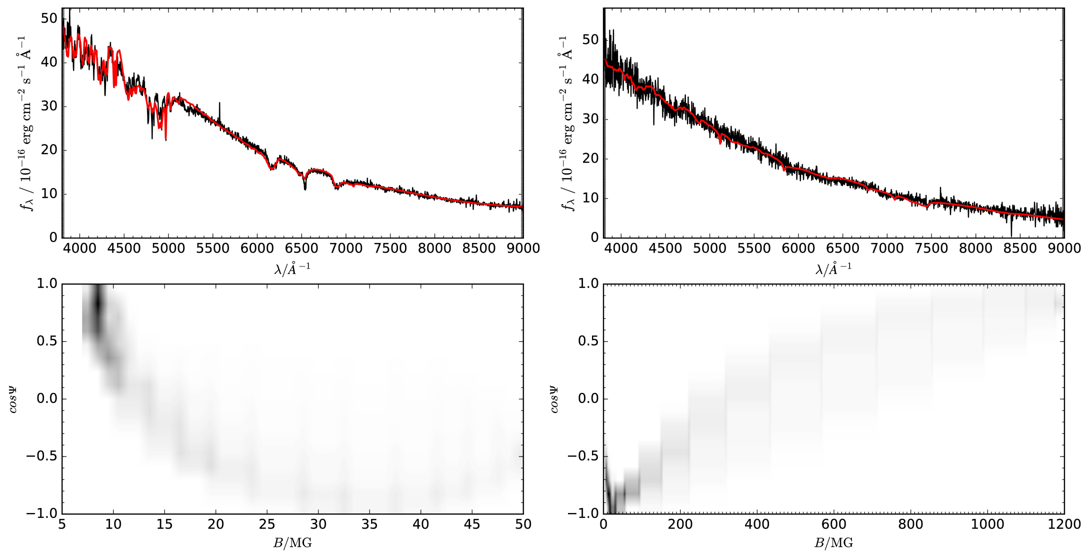

Figure 4.4: Two different spectra for the same star, showing drastic variability between the observations. The right spectrum is 1408-52822-0547 (S/N $\approx$ 16 in the g-band), from the Data Release 7, was well fitted with an off-centered dipole strength of $\sim$105 MG, while the left one, 5005-55751-0254 (S/N $\approx$ 36 in the same band), with only 35 MG.

This star seems to have passed from a weak field hemisphere, where Zeeman signatures can still be found, to a very high field one where all line profiles have vanished. Nevertheless, despite the high field solution and the low signal-to-noise of the right spectrum, some pretty shallow hydrogen lines can be identified far away from their zero-field position all along the continuum level (one of them is seen at $\lambda \approx 7500\mathring{A}$). Interestingly the two ZEBRA plots resemble one another quite well, except for a symmetrization in the $\cos\psi$ axis, but this is not important at all, beacuse the spectrum does not contain enough information for the code to distinguish between the flips of the dipole. In other words, he doesn't know whether is looking at north or south pole. However, they differ significantly in the range of fields that were used to build both models, as you can notice, in the case of 5005-55751-0254 (left) the model was build by superposing fields from 5 MG to 50 MG, each one with a different weight but with most dominat field at $\sim$ 8 MG (darker region), while the right one could only be fitted by diluting the field search in a much broader region: from 9 MG to 1200 MG, with dominant field close to 10 MG. Thus, the stellar face shown by the right spectrum is surprisingly more magnetized them the left one's. This phenomenon might have a nice solution which, again, does not take us too much further than the Solar System to provide us with good examples. But I don't want to tell you what it is until Sec. 4.2.

My advisor always says that a good theoretician must have at least three explanations for a certain unknown phenomenon. An when it comes to stellar magnetism, problems are sort of commonplace. Actually for us they sound like problems, reproduce it with the models and simulations can be hard, or even infeasible, but stars just do it quite easily, whatever it be. They often do in three seconds what a simulation in the biggest supercomputer in the world did in two years[2]! Stars just explode, burn, fuse, cool, merge, and they don't give a damn whether for us is difficult to understand it or not. Stars just do it! My advisor use to say that too. Well... hope not to disappoint him for having only one solution I have been working on all this time studying these problems. I shall finally turn out to present it to you in the next section, so keep up with me.

4.2 Dark spots

Dark spots are structures observed to freckle the surfaces of stars, including the Sun and white dwarfs [Kilic et al., 2015], and can basically be due to one of the two reasons below:

- **Metal channeling** When highly convective layers drag matter upwards the body of a star, it can carry some metals that used to dwell innermost depths. The flux of metals may form channels through which they flow towards the photosphere and build opaque localized regions, called chemical spots, that critically block part of the light path in relation to the surrounding. This gives the spots their lightless aspect[3].

- **Strong magnetic field** Magnetic fields might play an important role in the formation of dark spots, like they do in the Sun. The same convection that may create tunnels of metalic elements[4] up to the surface, and that becomes important for temperatures below $\sim$13000 K, also have the strength to curl magnetic field lines inside the very turbulent zones, like the water near the 100 °C you stare bubbling when cooking an egg. And thus the entangled field starts to increase in magnitude and suppress the natural matter flow, inhibiting convection to do its job and drag heated material from inner layers, plummeting temperature by some orders of magnitude. And through this temperature gradient (from inside to outside the spot place), it is easy to understand why of its black tone, since

[2] The most complex simulation ever done to study supernovae explosions really took all this long.

[3] Attention here! Don't let this information trick you. Although the lightless aspect is how we see dark spots, they are actually not black at all. A peace a sunspot isolated from the rest of the Sun would shine even brighter than the Moon! This effect is analogous to what is observed in the telescope when searching for extrasolar planets via planetary transit.

[4] Remember that, for us astronomers, metals are any elements other than hydrogen and helium.

you've probably met the famous equation relating luminosity to temperature of a heated black-body:

$$L = 4\pi\sigma R^2 T^4 \tag{4.1}$$

Thus, because of the fourth power dependence in temperature, even relatively small variations on T, entails huge variations on L, providing the star with a pair of dark blurs (remember $\nabla \cdot \mathbf{B} = 0$ abhors an existance of monopoles. So it must be a pair).

And by knowing this basic physics of convection, it was possible for me to think of an attempt of detecting evidences of surface spots in J030407. If convection really acts in order to form tangles with magnetic field lines, it will affect the way matter is transported along layers. And that, as explained before, inhibits heat to get upside and warm up top shells, causing the local temperature to decrease with respect to surroundings, making the star appear a some kelvins cooler in the hemisphere where the spot takes place. But the real size of the "some" depends on strength and size of the spot (at sunspots, the local temperature difference is around 5780 K).

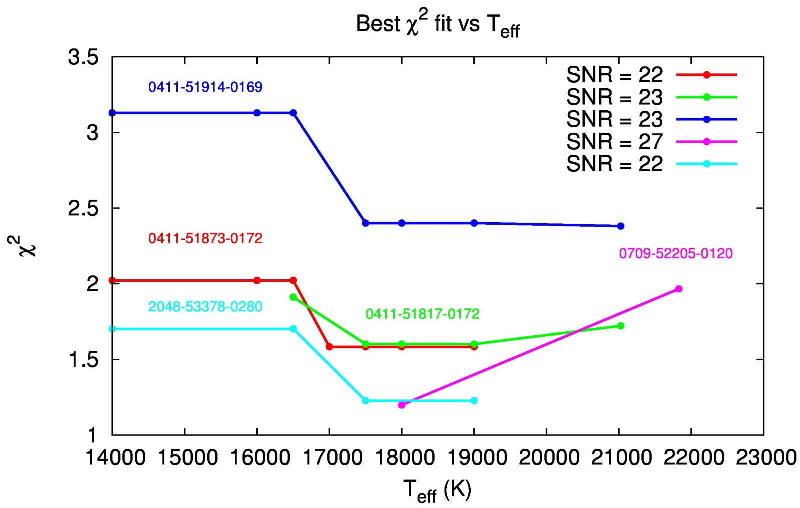

Figure 4.5: A χ^2 versus T_{eff} plot that shows runs for 5 different spectra from J030407 (the left plot). Only 5 because one of them have not converged to any of the trial fits I have done.

By fixing temperatures within a certain interval and setting other parameters as free, like the polar field strength (B_d), the z off-set (z_{off}) and the inclination, the code was ran a few times, to cover all spectra, with effective temperature assuming a different value in each execution. The χ^2 was computed as function of the trial temperatures, and the global minima solutions were obtained. In principle, and this was my start-up hypothesis, a dark spot would manifest itself by spreading the global solutions between different temperatures, *i.e.* each of the spectra would show a best-fit solution with a proper effective temperature, in a sense that the spotted face would have lower a T_{eff}, and the spot-free one would have higher T_{eff}. But all spectra seem to be well fitted with the same temperature. Does that mean that there is no spot at all? Actually not! It just ponts out that if the spot does really exist there, then it is too small to cause temperature differences in effective temperature. And this is no surprise, since the effective temperature of the Sun isn't affected, even when there are nearly 200 spots freckling the surface. Only the local temperature is changed. And you may wisely ask what is thus the minimum size for stellar spots to variate effective temperatures. This is a question for which I have no answer to give, but I think it's a nice problem for you to think about.

4.3 The lost link

About the thing I denied to tell you a few pages ago until this section, well, it's time! It has to do with Ap and Bp stars: as I was saying in Sec. 2.4, because of their off-set intrinsic characteristic, there is a wide discussion of whether these stars may be good candidates for the progenitors of magnetic white dwarfs. Moreover, they are curiously the only known main sequence stars to have globally organized magnetic fields, just like white dwarfs. But we still haven't found the real magnetic white dwarfs' ancestors, for many authors have already discussed this problem with yet uncertain conclusions [Kanaan et al., 1999,Külebi et al., 2009]. If this Ap- or Bp-to-white dwarf conversion does really happen in Nature, then the magnetic fields of white dwarfs might be a result of the evolutionary path traced by the field of those main sequence stars, and by that we can set our conclusions based on two distinct hypothesis that can be made about the field's nature. One of them predicates that the magnetic fields have a fossil origin, that reassembling to its earlier past while in the primordial cloud era. And if this is so, the magnetic field has a nuclear origin in the progenitors of white dwarfs (maybe Ap and Bp), and their magnetic fields may be connected somehow, differing only by an amplification factor that depends on the radius contraction scale, for what are white dwarfs if not nuclear remnants (you may call lumps) of dying stars after all? So this stellar metamorphosis from one type to another might occur through an extremely violent process of implosion in order to ampify the final field in some orders of magnitude. Remember the implosion technique used by Fowler (see Chap. 1) and think of it now in large scale. If we assume flux conservation, *i.e.* that during contraction the star does not lose part of its field because of ejected (magnetized) matter, this aplification factor might be 100 if the radius of the star diminish to a tenth of its initial size. Nevertheless, the truth is that we are not sure neither about this factor, nor if magnetic flux is really conserved during the implosion process. However, there are some authors doing attempts to investigate a second hypothesis, which is that the amazingly strong magnets hold by white dwarfs come from the intensive action of a dynamo mechanism sustaining its power during what is called a common envelope phase of binary interaction, where the field is largely amplified. This study was guided by magnetohydrodynamics simulations [Ohlmann et al., 2016].

4.4 Magnetic white dwarfs: from DA to DZ

Although the work here presented was concerning uniquely hydrogen-rich white dwarfs, Nature wouldn't hesitate to provide us with "stellar biodiversity", for the Universe contains myriads of stars, each of them with its own characteristics and peculiarities, like temperatures, colors, sizes, masses, chemical aboundancies, etc. Hydrogen, helium, carbon, oxigen, neon, magnesium, sodium, calcium. All essential ingredients of stellar boilers. Even some molecules like H_2^+ and olivine might be present [Jura et al., 2009]. In the stellar zoo, we find a variety of species indeed, but there are only a few atoms for which magnetism has been calculated, like hydrogen, helium, carbon, and some other metals. Hydrogen and helium, despite their low number of electrons, have an additional complicating factor, and that does not have strong effect on most metals, which is their very weak spin-orbit coupling. This factor, as the name says, keep the electron's intrinsic magnetic moment (spin) tightly bound to the orbital magnetic moment so they behave as a single being, which holds for a certain range until the field become strong enough to decouple them, and decoupling means to create more degrees of freedom, and more degrees of freedom mean more splitted components. There's still a lot of work to be done, in both theoretical and observational sides, for covering the gap left by the incomprehension of other atoms' magnetism. However, this scenario has been changing in recent years with the publication of brand new works devoted to study heavy elements in magnetic white dwarfs like [Hardy et al., 2016, Dufour et al., 2008]. Fig. 4.6 shows some examples of magnetic white dwarfs with heavy elements.

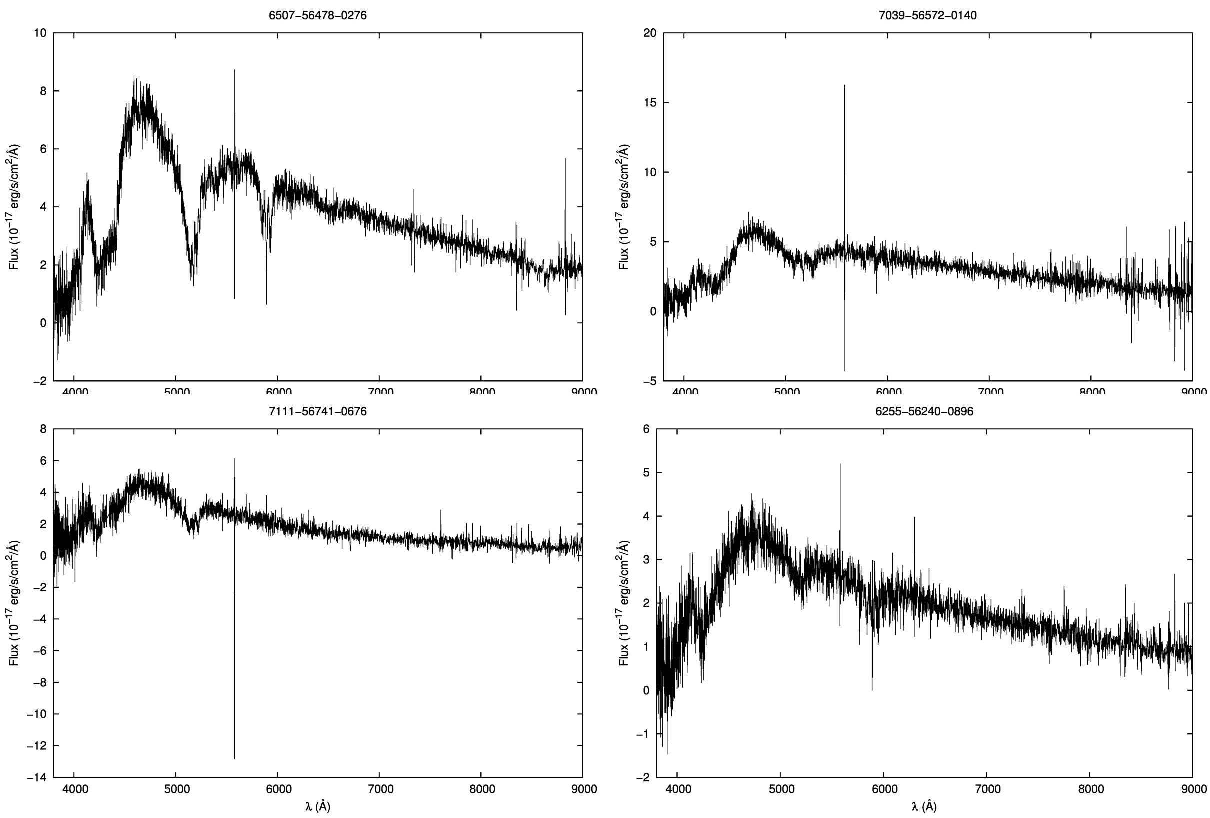

Figure 4.6: Metalic magnetic white dwarfs' spectra discovered by [Hollands et al., 2015]. Notice the Mg and NaD lines splitted by magnetic fields up to $\sim$ 10 MG.

Chapter 5

Conclusions and discussions

"We are drowning in information, but starved for knowledge"

— **John Neisbitt**

So long path of 36 pages about magnetism, white dwarf theory and observations to get to this very end, that I promisse this will be a shorter chapter.
In the very end, nearly 95% or so of all stars in the Milky Way will some day puff all their outer shells to left small, hot and compact lumps of burning matter called white dwarfs. In the very end, white dwarfs will cool down along several turns of the Sun around the Galaxy... billions of years to come. In the very end, one of the brightest explosions in the welkin shall feed its neighbors with the metals just-fused within the hearts of massive dying stars. This is how the Universe works. Universe of which magnetic fields are a part. Universe at which magnetic fields play an important character and still have a lot to teach us.
This study was thus devoted to investigate magnetic field's distribution among stellar surfaces of white dwarfs through the use of the numerical fitting routine called YAWP. This code was complemented by two other programs written by the author of this thesis that had significant importance to the former, one in C++ language (the same as YAWP) and the other in Python language. I was very lucky for thinking about starting to write the first program during my vacations, for it had helped to accelerate the acquirement of the calculated data by enormously increasing the frequency of the runs to several times faster, and the simuntaneity of them by enableling fits to be done in different processors on a computer at the same time. I apologyze with some of my friends for slowing down the efficiency of the computers I used to run my code. My program was also thought to smooth the local minima problem we discussed in Sec. 2.7 by beginning with different sets of start-up parameters in each run (remember the buckets game). However, even though the statistical study could be made without much trouble, the precise geometries of individual stars were intrinsically limited by the S/N ratio of our data, a limitation concerning mostly the field distribution, since the ZEBRA plots obtained for each spectrum are, in general, not unique. There could

be other field distributions with the same power of explaining the spectra we observe as the ones obtained before. And to this, there's not much we can do, we must learn to work in the context of what we have. In more sofisticated studies, like the series of papers by F. Euchner et al. [Euchner et al., 2002, Euchner et al., 2005, Euchner et al., 2006, Beuermann et al., 2007], where some of the Stokes parameters (like I and V) where measured to obtain an accurate polarimetry combined with phase-resolved spectra taken from one of the biggest ground-based telescopes of our time, the magnetic field becomes very well constrained, for one can do simuntaneous fits to all available data. Most of the ESO-VLT spectra they had reached significantly higher resolutions than ours. I believe to this work I had used at most 1/5 of YAWP's full power because of single-type data we have, with the advantage that the sample analyzed here was several times greater than the one used in F. Euchner's papers.
The second code, in Python, was only written later on, and was used for one of the last parts of my work, which was to calculate several F-statistics for comparing geometric models automatically. The routine I made was tested for consistency by being compared with the already stablished online platform `http://stattrek.com` for doing statistical tests and had lead to congruent results with respect to it. The code also had crucial relevance to better clearify the white dwarfs's field topologies, since due to this program I can say with all words here what I consider the most important conclusion in my thesis:

magnetic white dwarfs's field distributions are such that nearly 86% of the sample spectra show better fitted models by using off-centered dipoles, and somewhat simpler geometries are generally insufficient to explain the observations.

Nevertheless, everyone shall be aware that we may not afford ourselves to believe that there exist no false positives contaminating this number, because there safely are some, which by no means, can be separated from the true cases in the context of our data, since we lack more information about our stars to constrain the field distribution, like the polarimetry data obtained by F. Euchner et al. And at first you may be lead to think that this might be in disagreement with the fraction of Ap stars that are actually better adjusted with these off-sets, for almost one hundred per cent of them do fit better when off-setted. But I'm afraid this isn't correct, because you didn't realized that, curiously, there are some values of inclination (which was also a free parameters in all fits) of the dipole's magnetic moment hold by the star that are truely blind-spots to the off-sets, *i.e.* some configurations in which the field might be disposed will never show us the off-set, even if it is really there! Up to 33% of all possible inclination angles suffer from this blindness, highly depending on the data's signal-to-noise, and this number could provide us with the rest of the invisible better fits with off-sets, remembering that there are also the false positive cases which we have no ways of extracting from the results. So what I'm saying is that we may not discard the possibility of Ap stars to be the ancestors of magnetic white dwarfs, eventhough there remain some inconsistencies with that assumption, like the fact that there are more observed magnetic white dwarfs than the number of Ap can explain, and that's when we introduce the Bp in the candidates list. But think I've already said enough of my work for a while, after all, as Feynman would say: "I gotta stop somewhere, I'll leave you something to imagine".

Cosmology tells us we know only 5% of the Universe. So many things to know, so many ways we have, so few answers we've got. John Neisbitt was right. Although there's a long road until all the mysteries are solved (probably an endless road), I decided to dive into this Universe in order to give a tiny contribution, maybe discover something nice, and hopefully shade some light over the enigma, and I also took this as an opportunity to show you some of my personal beliefs. But I'm not in position of judging my achievements with this work, even because I suppose neither I, nor anyone else have actual conditions of probing what these objects are, where did they come from, and where are they going, for our current set of data is quite limited. Yet, I believe the Universe does hold the key-answers to all our questions, and just like a sea shell holding a pearl, in order to reveal its secrets it is necessary to open it and look inside. And that's what makes science so exciting, no matter how sharpened our vision is, there will always be secrets to find out, and questions do be made.

And to finish this once and for all, I'd like to end this thesis confessing myself of really having enjoyed spending my time writing about an issue that I do love with the best of my astrophysical heart, and that I spent very pleasureful hours thinking of better ways to present the concepts here so you could feel the same way I do with magnetic fields, white dwarfs, and physics as a whole. But you're the only one that can say if I was successful. Now, I know what you are thinking! You are thinking of that standard question that every astronomer likes to do. A simple question that can be summarized in: what is the purpose of studying these stars? If I was successful in guessing that you are really thinking of it at this moment (or at least if I induced you to think of it now), let me give you a simple answer, or... even better, let me say that this is a question for which "the prince of the poets", Olavo Bilac, would have an adequate answer with a little modification to english:

"Do love to understand them, for only the one who loves has ears capable of hearing and understand stars".

Chapter 6

APPENDIX

6.1 Linear Zeeman effect: semi-classical approach

In order to describe linear Zeeman effect, it is not necessary to use quantum mechanics in its full power. Instead, we might prefer a semi-classical approach, which means borrowing some aspects of classical mechanics to do so. First, consider a two-body problem with hamiltonian $\mathcal{H}_0$ where an electron (charge $-e$) is orbiting a proton (charge $+e$) under the influence of an external, uniform magnetic field $\mathbf{B}$. In the presence of that field, the original hamiltonian needs a correction due to the energy sustained by $\mathbf{B}$. In other words, we simply sum $\mathcal{H}_m$, the energy carried by the magnetic field itself, to $\mathcal{H}_0$, giving birth to the new total energy of the system: $\mathcal{H} = \mathcal{H}_0 + \mathcal{H}_m$. Classically, we expect the electron's orbiting around the proton to behave like a very simple electric circuit where the current flow carries a charge $-e$. And by the right-hand rule, the current also possesses a natural magnetic moment $\mathbf{M}$ orthogonal to the circulation plane due to the charge motion. Why am I saying that? Because we can write the hamiltonian (energy, if you prefer) carried by the magnetic field in terms of $\mathbf{M}$ and $\mathbf{B}$ in a very compact form:

$$\mathcal{H}_m = -\mathbf{M} \cdot \mathbf{B} \tag{6.1}$$

From classical electrodynamics, an electric current I circulating within a loop enclosing an area A has a magnetic moment given by: $\mathbf{M} = I\mathbf{A}$, where $\mathbf{A}$ is the area vector, with modulus A and direction perpendicular to the loop plane. Let the unitary vector $\mathbf{u}$ point towards this direction. For the case of a circular loop of radius R: $\mathbf{M} = I\mathbf{A} = I\pi R^2\mathbf{u}$. Using the chain rule in the definition of current:

$$I \equiv \frac{\mathrm{d}q}{\mathrm{d}t} = \frac{\mathrm{d}q}{\mathrm{d}x}\frac{\mathrm{d}x}{\mathrm{d}t} = \frac{\mathrm{d}q}{\mathrm{d}x}v \tag{6.2}$$

Assuming a uniform current distribution all over the loop, we may interchange the charge spatial derivative by a simple fraction of the total quantities:

$$I = \frac{\mathrm{d}q}{\mathrm{d}x}v = \frac{q}{x}v = \frac{q}{2\pi R}v \therefore M = \pi R^2 \frac{q}{2\pi R}v = \frac{qRv}{2} \tag{6.3}$$

By writing v in terms of the orbital angular momentum of the electron's circular orbit ($\mathbf{L} = m_e v R \mathbf{u}$) and comparing it with the expression just derived above, making $q = -e$:

$$\mathbf{M} = -\frac{eR}{2}\left(\frac{\mathbf{L}}{m_e R}\right) = -\frac{e}{2m_e}\mathbf{L} \tag{6.4}$$

From Eq.(6.4), it turns out that the hamiltonian from Eq.(6.1) can be written as:

$$\mathcal{H}_m = \frac{e}{2m_e}\mathbf{B} \cdot \mathbf{L} \tag{6.5}$$

Physicists use to call $\lambda_e \equiv -e/2m_e$ the **gyromagnetic factor** of the electron, because of its quite simple interpretation. A fast glance at the very right side of Eq.(6.4) leads you to write it as: $\mathbf{M} = \lambda_e \mathbf{L}$. So λ_e measures how much $\mathbf{M}$ is coupled to rotation, whose role is played by the angular momentum. In other words, because λ_e depends on the magnitude of q, it describes how a spinning charge (electron) retains dipole magnetic moment from its orbital angular momentum.

Now, without any loss in generality, we may choose a reference frame such that the magnetic field vector is aligned with the z-axis. In this frame:

$$\mathcal{H}_m = \frac{e}{2m_e}BL_z \tag{6.6}$$

The quantum mechanical analogue of that expression is straightfoward, just replace $\mathcal{H}$ and L_z by their operational forms (put a hat on them), and apply the total hamiltonian to a state vector, let's say $|\psi\rangle$, remembering the eigenvalue spectrum for the angular momentum's z component $\hat{L}_z |\psi\rangle = m\hbar |\psi\rangle$:

$$(\hat{\mathcal{H}}_0 + \hat{\mathcal{H}}_m)|\psi\rangle = \hat{\mathcal{H}}_0 |\psi\rangle + \frac{e}{2m_e}B(\hat{L}_z|\psi\rangle) = E_n|\psi\rangle + \frac{e}{2m_e}B(m\hbar|\psi\rangle) = \left[E_n + \left(\frac{e\hbar}{2m_e}\right)mB\right]|\psi\rangle \tag{6.7}$$

Recognizing the factor $e\hbar/2m_e$ as Bohr's magneton μ_B, we finally arrive to the expression for the atom's energy levels in linear regime of Zeeman effect:

$$\boxed{E = E_n + \mu_B m B} \tag{6.8}$$

This formula explains the three-level pattern of spectral lines within the weak field regime. And the first order approximation to the wavelength shift can also be calculated as [Preston, 1970]:

$$\Delta\lambda_l = \pm 4.67 \times 10^{-13}\lambda^2 B \tag{6.9}$$

where the subscript l stands for "linear". λ is measured in $\mathring{A}$, and B in MG. The linear dependence with the field marks the signatures of normal the normal Zeeman effect. However, if the field is strong enough (greater than $\sim$ 10 MG), higher-order terms shall be accounted, for the shifts start to deviate from linearity. It can be shown that the quadratic Zeeman displacement is given by [Jenkins and Segre, 1939]:

$$\Delta\lambda_q = -\frac{e^2}{a_0^2} 8 m_e c^3 h \lambda^2 n^4 (1 + k^2) B^2 \tag{6.10}$$

where the subscript q stands for "quadratic". In this equation, a_0 is the Bohr radius, n is the principal quantum number, and $k \equiv m_l + m_s$ is the magnetic quantum number.

6.2 Output data

PMF	χ^2	$T_{\rm eff}$ (K)	B (MG)	u_B (MG)	$z_{\rm off}$	$u_{\rm offset}$	incl. (°)	$u_{\rm incl}$ (°)
0283-51584-0120	10.13	17000	2.22	∞	0.17	∞	0.54	∞
0337-51997-0264	1.69	18000	8.69	∞	-0.08	∞	83.76	∞
0359-51821-0415	6.17	10157	36.95	∞	-0.05	∞	53.09	∞
0366-52017-0591	21.73	10818	2.98	∞	0.36	∞	0	∞
0373-51788-0086	3.95	29770	2.31	1.7	-0.18	0.22	76.28	60
0373-51788-0243	72.24	32204	5.51	∞	0.30	∞	0	∞
0374-51791-0583	4.86	12239	113.37	∞	-0.25	∞	15.71	∞
0411-51817-0172	1.71	21026	11.06	2.1	-0.02	093	58.98	18
0416-51811-0590	3.70	8000	2.29	0.79	-0.27	0.046	10.57	9.8
0437-51869-0369	0.47	10080	64.96	∞	-0.31	∞	1.41	∞
0503-51999-0244	0.73	10108	126.99	∞	-0.11	∞	58.31	∞
0542-51993-0639	291.84	39100	19.98	∞	0.22	∞	0.00	∞
0564-52224-0248	4.89	8000	4.24	0.78	-0.11	0.031	0.20	0.1
0580-52368-0274	2.63	8000	2.14	0.78	-0.11	0.036	49.16	23
0594-52045-0400	6.95	15760	3.79	∞	-0.43	∞	2.16	∞
0710-52203-0311	31.51	19945	16.88	∞	0.49	∞	3.92	∞
0733-52207-0522	3.53	22904	16.37	3.8	0.08	0.018	25.24	13
0757-52238-0144	2.12	12930	32.13	∞	-0.46	∞	37.91	∞
0818-52395-0026	2.33	17872	2.01	0.0	-0.12	0.14	20.69	16
0885-52379-0319	30.59	8183	2.20	∞	-0.49	∞	0.19	∞
0901-52641-0373	3.48	8946	4.15	1	-0.28	0.066	6.85	23
0966-52642-0474	1.52	20160	5.05	1	-0.25	0.084	62.88	43
1193-52652-0481	0.98	23420	9	2.3	-0.10	0.056	64.70	40
1200-52668-0538	2.33	10108	42.29	6.5	-0.13	0.068	51.61	31
1215-52725-0241	4.26	10985	3.02	0.0	-0.47	0.089	57.03	23
1221-52751-0177	6.74	18997	2.55	∞	-0.27	∞	58.49	∞
1222-52763-0477	14461	14306	2.41	∞	0.31	∞	0.38	∞
1222-52763-0625	4.37	10537	3.58	5.4	0.50	0.16	2.28	1.1
1228-52728-0220	6.42	8000	2.02	∞	-0.11	∞	0.20	∞
1237-52762-0533	5.42	8000	2.06	∞	-0.30	∞	0.32	∞
1311-52765-0421	6.39	10080	3.42	∞	0.50	∞	2.22	∞
1408-52822-0547	2.01	11000	105.78	∞	-0.29	∞	21.74	∞
1451-53117-0582	3.72	9790	5.91	1.9	-0	0.011	19.28	29
1452-53112-0181	3.92	10100	22.77	2.6	-0.22	0.056	52.02	30

PMF	χ^2	$T_{\rm eff}$ (K)	B (MG)	u_B (MG)	$z_{\rm off}$	$u_{\rm offset}$	incl. (°)	$u_{\rm incl}$ (°)
1456-53115-0190	2.80	8000	4.22	0.8	-0.11	0.032	0.20	0.1
1616-53169-0423	1.76	8544	2.37	0.42	-0.07	0.012	42.39	16
1622-53385-0447	5.14	9888	2.29	0.59	-0.27	0.068	42.86	24
1663-52973-0119	7.45	32204	3.30	∞	0.32	∞	31.24	∞
1699-53148-0137	12.24	8000	2.31	∞	-0.08	∞	44.02	∞
1709-53533-0511	3.66	8000	2.05	0.0	-0.11	0.031	0.20	0.1
1770-53171-0530	3.50	10082	18.40	2.1	-0.03	079	52.78	11
1798-53851-0233	0.46	40000	12.41	∞	-0.36	∞	37.38	∞
1837-53494-0261	0.30	8000	104.02	∞	-0.30	∞	8.80	∞
1907-53315-0427	70.86	10676	2.91	∞	0.42	∞	0.09	∞
1933-53381-0151	1.78	10815	160.91	17	-0.19	0.065	58.98	32
1953-53358-0415	8.45	14462	2.29	∞	-0.27	∞	57.77	∞
1989-53772-0041	0.65	25365	6.15	1.9	0.00	0.00	57.35	36
2006-53476-0332	0.62	38124	22.22	0.0	0.30	0.19	22.32	20
2046-53327-0048	1.35	12986	166.30	30	-0.18	0.057	43.69	23
2049-53350-0450	0.87	23000	11.69	3.9	-0.06	0.022	49.79	23
2063-53359-0272	23.99	21035	2.43	∞	0.17	∞	0.36	∞
2072-53430-0336	62.60	16444	1.65	∞	0.10	∞	71.10	∞
2081-53357-0442	1.89	10135	36.34	7.4	-0.10	0.06	0.32	0.33
2082-53358-0444	3.64	8000	2.01	∞	-0.11	∞	0.20	∞
2131-53819-0317	1.46	9906	2.13	1.1	-0.11	0.054	67.06	33
2134-53876-0423	1.53	8000	20.17	0.0	-0.18	0.039	44.10	36
2156-54525-0031	109.47	19850	3.34	∞	0.33	∞	0.12	∞
2169-53556-0491	4.87	9732	2.29	0.63	-0.27	0.088	53.79	28
2258-54328-0295	51.17	18529	2.75	∞	0.24	∞	0.00	∞
2265-53674-0033	0.98	12347	35.76	17	-0.44	0.13	29.05	38
2292-53713-0019	4.82	13277	62.76	7.4	-0.14	0.044	60.19	30
2310-53710-0420	0.79	45000	29.38	∞	0.46	∞	23.91	∞
2319-53763-0209	2.27	15584	2.29	0.77	-0.27	0.089	71.59	42
2320-54653-0445	12.71	25075	2.10	∞	0.08	∞	5.66	∞
2644-54210-0167	1.58	15144	2.03	0.0	-0.10	0.046	80.60	41
3183-54833-0179	3.84	8000	2.31	0.45	-0.08	0.014	44.17	27
3660-55209-0322	1.51	37086	30.00	8.2	0.04	0.1	4.07	11
3670-55480-0528	11.99	8000	2.14	∞	-0.11	∞	49.12	∞
3676-55186-0030	2.85	22420	2.06	0.0	-0.10	0.032	20.39	6.2
3775-55207-0698	0.62	10198	24.67	5.4	-0.28	0.12	46.53	33
3813-55532-0364	1.22	30361	20.09	0.0	0.13	0.12	66.21	37
3852-55243-0676	0.49	31128	13.36	3.8	-0.13	0.097	58.45	44
3947-55332-0016	0.75	23954	8.37	0.0	-0.20	0.13	75.38	46
3962-55660-0428	0.53	45000	20.66	∞	-0.06	∞	77.60	∞
4006-55328-0358	2.27	18462	2.11	∞	0.16	∞	0.14	∞
4023-55328-0122	2.04	14626	2.26	∞	0.31	∞	89.62	∞
4061-55362-0761	0.85	21603	2.56	1.1	-0.30	0.18	17.75	13
4223-55451-0634	5.72	18764	2.05	0.0	-0.10	0.03	50.26	55

PMF	χ^2	$T_{\rm eff}$ (K)	B (MG)	u_B (MG)	$z_{\rm off}$	$u_{\rm offset}$	incl. (°)	$u_{\rm incl}$ (°)
4286-55499-0125	0.71	30000	2.58	0.0	-0.38	0.27	66.94	51
4443-55539-0256	0.33	9750	110.59	20	-0.05	0.05	65.02	57
4468-55894-0368	0.61	35245	2.81	0.0	0.41	0.54	76.25	78
4484-55565-0072	1.94	18218	2.88	0.7	-0.21	0.069	49.82	75
4505-55603-0384	0.74	12347	29.05	∞	-0.26	∞	7.92	∞
4534-55863-0248	0.42	9000	12.96	4.9	-0.47	0.16	42.46	32
4568-55600-0952	0.54	17000	64.48	10	-0.31	0.11	67.52	46
4713-56044-0230	3.59	30000	9.86	∞	0.18	∞	8.97	∞
4772-55654-0128	0.96	23045	11.68	2.8	0.04	0.083	85.09	37
4786-55651-0518	5.25	17415	2.19	0.97	-0.10	0.031	63.16	27
4808-55705-0466	0.68	23000	40.53	13	-0.07	0.043	54.56	41
4855-55926-0376	1.97	11000	14.79	2.7	-0.10	0.024	72.15	31
4878-55710-0747	1.29	30000	33.87	9.8	0.14	0.06	37.21	150
4890-55741-0988	0.41	38240	2.29	4.5	-0.27	0.15	65.14	59
4901-55711-0358	0.96	24000	2.16	1	0.12	0.12	33.15	26
4975-56037-0762	2.50	37472	9.48	∞	-0.49	∞	51.73	∞
4976-56046-0553	1.65	17750	21.61	0.0	-0.29	0.12	79.30	30
4988-55825-0107	0.68	23491	2.76	2.5	-0.27	0.31	42.72	30
5005-55751-0254	0.81	11000	34.99	4.1	-0.16	0.05	59.16	48
5167-56066-0732	0.56	29032	20.38	0.0	0.12	0.072	79.66	38
5198-55823-0511	1.85	17872	2.15	0.85	-0.10	0.033	20.40	11
5299-55927-0834	0.80	45000	73.27	∞	-0.41	∞	19.65	∞
5368-56001-0206	1.49	12591	135.52	36	-0.19	0.062	2.26	6
5371-55976-0512	0.99	8000	257.94	∞	0.13	∞	15.12	∞
5389-55953-0671	2.95	8000	2.08	0.0	-0.11	0.031	0.20	0.1
5393-55946-0981	0.87	20024	2.26	∞	-0.27	∞	2.78	∞
5426-55987-0342	0.19	40000	13.02	∞	-0.24	∞	44.32	∞
5736-55984-0466	1.81	18625	2.10	0.0	-0.09	0.035	46.24	23
5786-56251-0182	2.10	13277	61.06	6.1	-0.14	0.028	62.45	27
5869-56064-0446	1884.75	11413	245.72	∞	0.28	∞	21.88	∞
5892-56035-0686	0.85	19858	2.17	∞	-0.10	∞	63.86	∞
5942-56210-0336	1.37	37086	29.94	7.6	0.03	0.025	0.0	2.4
5964-56098-0187	5.08	8000	2.31	0.41	-0.08	0.013	44.02	24
5974-56314-0382	1.73	15144	2.06	0.0	-0.11	0.23	73.65	62
6013-56074-0656	2.01	17803	2.01	0.0	0.09	0.078	34.78	19

PMF	χ^2	$T_{\rm eff}$ (K)	B (MG)	u_B (MG)	$z_{\rm off}$	$u_{\rm offset}$	incl. (°)	$u_{\rm incl}$ (°)
6027-56103-0970	1.47	34687	17.01	5	-0.0	0.016	45.37	31
6054-56089-0954	1.19	11000	8.41	0.0	-0.25	0.058	5.48	18
6299-56478-0639	0.87	9124	8.31	∞	-0.25	∞	9.03	∞
6421-56274-0804	0.99	9000	80.80	8.9	0.21	0.045	89.42	37
6518-56567-0796	0.68	22000	5.00	2	-0.47	0.21	32.46	40
6619-56371-0368	22.10	37375	3.99	∞	0.50	∞	9.62	∞
6635-56370-0334	0.81	11000	26.91	24	-0.49	0.15	18.35	25
6678-56401-0952	3.47	30000	2.15	∞	-0.29	∞	55.47	∞
6683-56416-0330	8.88	9157	13.17	∞	-0.40	∞	55.82	∞
6744-56399-0957	1.88	16628	2.98	0.0	0.44	0.39	39.04	0.0
6746-56386-0678	4.73	22165	11.54	∞	-0.02	∞	79.30	∞
6828-56430-0780	2.15	17136	2.13	0.0	-0.31	0.087	2.55	2
7083-56722-0200	1.50	25142	46.30	∞	-0.35	∞	39.23	∞
7103-56661-0066	1.85	25000	7.74	3.8	-0.40	0.29	63.15	48
7106-56663-0100	1.73	10687	14.82	2.1	-0.39	0.069	44.17	100
7106-56663-0132	4.52	23375	14.81	3.2	-0.13	0.047	44.18	28
7120-56720-0426	0.60	20000	24.96	10	-0.45	0.26	56.75	51
7167-56604-0030	1.21	30000	10.47	6.8	-0.44	0.21	52.23	50

Table 6.1: Output calculations with off-centered dipole as input geometry for each free parameter and uncertainties in the models of all spectra for which models have converged. Some of they didn't, and so we couldn't find any reasonable solution. The infinities in the table indicate that errors where not obtained in that particular case. If something seem weird to you, like zero uncertainty, nevermind, for some of them are only numerical estimations of the internal uncertainty and not the systematic one.

Bibliography

[Beuermann et al., 2007] Beuermann, K., Euchner, F., Reinsch, K., Jordan, S., and Gänsicke, B. T. (2007). Zeeman tomography of magnetic white dwarfs-iv. the complex field structure of the polars ef eridani, bl hydri and cp tucanae. *Astronomy & Astrophysics*, 463(2):647–655.

[Brinkworth et al., 2013] Brinkworth, C. S., Burleigh, M. R., Lawrie, K., Marsh, T. R., and Knigge, C. (2013). Measuring the rotational periods of isolated magnetic white dwarfs. *The Astrophysical Journal*, 773(1):47.

[Chandrasekhar and Fermi, 1953] Chandrasekhar, S. and Fermi, E. (1953). Problems of gravitational stability in the presence of a magnetic field. *The Astrophysical Journal*, 118:116.

[Chanmugam and Gabriel, 1972] Chanmugam, G. and Gabriel, M. (1972). Magnetic fields of white dwarfs. *Astronomy and Astrophysics*, 16:149.

[Coelho et al., 2014] Coelho, J., Marinho, R., Malheiro, M., Negreiros, R., Cáceres, D., Rueda, J., and Ruffini, R. (2014). Dynamical instability of white dwarfs and breaking of spherical symmetry under the presence of extreme magnetic fields. *The Astrophysical Journal*, 794(1):86.

[Donati et al., 1994] Donati, J., Achilleos, N., Matthews, J., and Wesemael, F. (1994). Zebra-zeeman broadening analysis of magnetic white dwarfs i. maximum entropy reconstruction of halpha profiles. *Astronomy and Astrophysics*, 285:285–299.

[Dufour et al., 2008] Dufour, P., Fontaine, G., Liebert, J., Schmidt, G. D., and Behara, N. (2008). Hot dq white dwarfs: something different. *The Astrophysical Journal*, 683(2):978.

[Euchner et al., 2002] Euchner, F., Jordan, S., Beuermann, K., Gänsicke, B., and Hessman, F. (2002). Zeeman tomography of magnetic white dwarfs-i. reconstruction of the field geometry from synthetic spectra. *Astronomy & Astrophysics*, 390(2):633–647.

[Euchner et al., 2006] Euchner, F., Jordan, S., Beuermann, K., Reinsch, K., and Gänsicke, B. (2006). Zeeman tomography of magnetic white dwarfs. *Astronomy and Astrophysics*, 451(2):671–681.

[Euchner et al., 2005] Euchner, F., Reinsch, K., Jordan, S., Beuermann, K., and Gaensicke, B. T. (2005). Zeeman tomography of magnetic white dwarfs-ii. the quadrupole-dominated magnetic field of he 1045-0908. *Astronomy & Astrophysics*, 442(2):651–660.

[Ferrario et al., 2015] Ferrario, L., de Martino, D., and Gänsicke, B. T. (2015). Magnetic white dwarfs. *Space Science Reviews*, 191(1-4):111–169.

[Fowler et al., 1960] Fowler, C., Garn, W., and Caird, R. (1960). Production of very high magnetic fields by implosion. *Journal of Applied Physics*, 31(3):588–594.

[Gentile Fusillo et al., 2017] Gentile Fusillo, N., Tremblay, P.-E., Jordan, S., Gänsicke, B., Kalirai, J., and Cummings, J. (2017). Can magnetic fields suppress convection in the atmosphere of cool white dwarfs? a case study on wd2105- 820. *Monthly Notices of the Royal Astronomical Society*, 473(3):3693–3699.

[Hardy et al., 2016] Hardy, F., Dufour, P., and Jordan, S. (2016). Magnetic white dwarfs with heavy elements. *arXiv preprint arXiv:1610.01522*.

[Hollands et al., 2015] Hollands, M., Gänsicke, B., and Koester, D. (2015). The incidence of magnetic fields in cool dz white dwarfs. *Monthly Notices of the Royal Astronomical Society*, 450(1):681–690.

[Jenkins and Segre, 1939] Jenkins, F. and Segre, E. (1939). The quadratic zeeman effect. *Physical Review*, 55(1):52.

[Jura et al., 2009] Jura, M., Farihi, J., and Zuckerman, B. (2009). Six white dwarfs with circumstellar silicates. *The Astronomical Journal*, 137(2):3191.

[Kanaan et al., 1999] Kanaan, A., Claver, C., and Liebert, J. (1999). The origin of strong magnetic fields in white dwarfs. In *11th European Workshop on White Dwarfs*, volume 169, page 221.

[Kapitza, 1924] Kapitza, P. L. (1924). α-ray tracks in a strong magnetic field. *Proceedings of the Royal Society of London. Series A, Containing Papers of a Mathematical and Physical Character*, 106(739):602–622.

[Kepler et al., 2016a] Kepler, S., Koester, D., and Ourique, G. (2016a). A white dwarf with an oxygen atmosphere. *Science*, 352(6281):67–69.

[Kepler et al., 2014] Kepler, S. O., Pelisoli, I., Koester, D., Ourique, G., Kleinman, S. J., Romero, A. D., Nitta, A., Eisenstein, D. J., Costa, J. E. d. S., Külebi, B., et al. (2014). New white dwarf stars in the sloan digital sky survey data release 10. *Monthly Notices of the Royal Astronomical Society*, 446(4):4078–4087.

[Kepler et al., 2016b] Kepler, S. O., Pelisoli, I., Koester, D., Ourique, G., Romero, A. D., Reindl, N., Kleinman, S. J., Eisenstein, D. J., Valois, A. D. M., and Amaral, L. A. (2016b). New white dwarf and subdwarf stars in the sloan digital sky survey data release 12. *Monthly Notices of the Royal Astronomical Society*, 455(4):3413–3423.

[Kilic et al., 2015] Kilic, M., Gianninas, A., Bell, K. J., Curd, B., Brown, W. R., Hermes, J., Dufour, P., Wisniewski, J. P., Winget, D., and Winget, K. (2015). A dark spot on a massive white dwarf. *The Astrophysical Journal Letters*, 814(2):L31.

[Kleinman et al., 2012] Kleinman, S. J., Kepler, S. O., Koester, D., Pelisoli, I., Peçanha, V., Nitta, A., Costa, J. E. d. S., Krzesinski, J., Dufour, P., Lachapelle, F.-R., et al. (2012). Sdss dr7 white dwarf catalog. *The Astrophysical Journal Supplement Series*, 204(1):5.

[Kleinman et al., 2013] Kleinman, S. J., Kepler, S. O., Koester, D., Pelisoli, I., Peçanha, V., Nitta, A., Costa, J. E. d. S., Krzesinski, J., Dufour, P., Lachapelle, F.-R., et al. (2013). Sdss dr7 white dwarf catalog. *The Astrophysical Journal Supplement Series*, 204(1):5.

[Koester, 2010] Koester, D. (2010). White dwarf spectra and atmosphere models. *Memorie della Societa Astronomica Italiana*, 81:921–931.

[Koester, 2015] Koester, D. (2015). *White Dwarfs Stars*.

[Koester et al., 1998] Koester, D., Dreizler, S., Weidemann, V., and Allard, N. (1998). Search for rotation in white dwarfs. *Astronomy and Astrophysics*, 338:612–622.

[Külebi et al., 2009] Külebi, B., Jordan, S., Euchner, F., Gaensicke, B. T., and Hirsch, H. (2009). Analysis of hydrogen-rich magnetic white dwarfs detected in the sloan digital sky survey. *Astronomy & Astrophysics*, 506(3):1341–1350.

[Landstreet et al., 2016] Landstreet, J., Bagnulo, S., Martin, A., and Valyavin, G. (2016). Discovery of an extremely weak magnetic field in the white dwarf ltt 16093= wd 2047+ 372. *Astronomy & Astrophysics*, 591:A80.

[Landstreet et al., 2017] Landstreet, J., Bagnulo, S., Valyavin, G., and Valeev, A. (2017). Monitoring and modelling of white dwarfs with extremely weak magnetic fields-wd 2047+ 372 and wd 2359-434. *Astronomy & Astrophysics*, 607:A92.

[Mestel, 1965] Mestel, L. (1965). Stellar structure. *Stars and Stellar Systems*, 8:465.

[Ohlmann et al., 2016] Ohlmann, S. T., Röpke, F. K., Pakmor, R., Springel, V., and Müller, E. (2016). Magnetic field amplification during the common envelope phase. *Monthly Notices of the Royal Astronomical Society: Letters*, 462(1):L121–L125.

[Preston, 1970] Preston, G. W. (1970). The quadratic zeeman effect and large magnetic fields in white dwarfs. *The Astrophysical Journal*, 160:L143.

[Putney and Jordan, 1995] Putney, A. and Jordan, S. (1995). Off-centered dipole models for three isolated magnetic white dwarfs. *The Astrophysical Journal*, 449:863.

[Rusomarov et al., 2017] Rusomarov, N., Kochukhov, O., and Lundin, A. (2017). Magnetic field topology and chemical spot distributions of the ap star hd119419. *arXiv preprint arXiv:1710.04396*.

[Schimeczek and Wunner, 2014] Schimeczek, C. and Wunner, G. (2014). Atomic data for the spectral analysis of magnetic da white dwarfs in the sdss. *The Astrophysical Journal Supplement Series*, 212(2):26.

[Tremblay et al., 2015] Tremblay, P.-E., Fontaine, G., Freytag, B., Steiner, O., Ludwig, H.-G., Steffen, M., Wedemeyer, S., and Brassard, P. (2015). On the evolution of magnetic white dwarfs. *The Astrophysical Journal*, 812(1):19.

[Tremblay et al., 2013] Tremblay, P.-E., Ludwig, H.-G., Steffen, M., and Freytag, B. (2013). Pure-hydrogen 3d model atmospheres of cool white dwarfs. *Astronomy & Astrophysics*, 552:A13.

[Valeev et al., 2017] Valeev, A., Antonyuk, K., Pit, N., Moskvitin, A., Grauzhanina, A., Gadelshin, D., Kolesnikov, S., Zhuzhulina, E., Burlakova, T., Galazutdinov, G., et al. (2017). Search for and study of photometric variability in magnetic white dwarfs. *Astrophysical Bulletin*, 72(1):44–50.

[Valyavin et al., 2014] Valyavin, G., Shulyak, D., Wade, G., Antonyuk, K., Zharikov, S., Galazutdinov, G., Plachinda, S., Bagnulo, S., Machado, L. F., Alvarez, M., et al. (2014). Suppression of cooling by strong magnetic fields in white dwarf stars. *Nature*, 515(7525):88–91.

[Vanlandingham et al., 2005] Vanlandingham, K. M., Schmidt, G. D., Eisenstein, D. J., Harris, H. C., Anderson, S. F., Hall, P. B., Liebert, J., Schneider, D. P., Silvestri, N. M., Stinson, G. S., et al. (2005). Magnetic white dwarfs from the sdss. ii. the second and third data releases. *The Astronomical Journal*, 130(2):734.

[Wickramasinghe and Ferrario, 2005] Wickramasinghe, D. and Ferrario, L. (2005). The origin of the magnetic fields in white dwarfs. *Monthly Notices of the Royal Astronomical Society*, 356(4):1576–1582.